[American Journal of Science, Vol. 300, April, 2000, P. 251–288]

American Journal of Science

APRIL 2000

AGE AND MAGMATIC HISTORY OF THE ANTANANARIVO BLOCK, CENTRAL MADAGASCAR, AS DERIVED FROM ZIRCON GEOCHRONOLOGY AND ND ISOTOPIC SYSTEMATICS

ALFRED KRÖNER*, ERNST HEGNER**, ALAN S. COLLINS***, BRIAN F. WINDLEY****, TIMOTHY S. BREWER****, THEODORE RAZAKAMANANA*****, and ROBERT T. PIDGEON******

ABSTRACT. We report single zircon $^{207}Pb/^{206}Pb$ evaporation and SHRIMP ages, combined with whole-rock Nd isotopic systematics for granitoid rocks from the Antananarivo Block (terrane), one of five tectono-metamorphic units making up the Precambrian basement of central and northern Madagascar. Our data reveal three distinct age groups at ~560 to 530, ~820 to 720, and 2520 to 2500 Ma respectively that reflect major magmatic events and correlate with similar events in various parts of East Africa and Sri Lanka but not in southwestern India. A widespread high-grade metamorphic event at ~550 Ma transformed many of the earlier granitoid gneisses into enderbite-charnockite assemblages. This granulite-facies event is common to Madagascar, East Africa, and southernmost India/Sri Lanka and reflects the final amalgamation of East and West Gondwana. Contrary to previous interpretations, there is a distinct lack of Kibaran-Grenvillian magmatism or metamorphism in Madagascar, making it unlikely that the island played a major role in the accretionary history and amalgamation of the supercontinent Rodinia.

The widespread and voluminous granitoid magmatism at ~824 to 720 Ma remains enigmatic, and the tectonic scenario with which it is associated is difficult to reconstruct due to severe tectonic transposition of most gneisses. The Nd isotopic systematics as well as abundant zircon xenocrysts attest to extensive remelting of Archean and Paleoproterozoic crust. On presently available data the ~740 to 820 Ma granitoids are either related to magmatic underplating following plume generation, subcrustal mantle delamination during break-up and dispersal of Rodinia, or to continental arc magmatism related to subduction of the Mozambique ocean. They were emplaced into the ancient crust of central Madagascar as it lay either attached to East Africa or formed a microcontinent within the Mozambique ocean.

INTRODUCTION

The East African orogen (Stern, 1994; Meert and Van der Voo, 1997) includes the low grade terrains of the Arabian-Nubian shield in the north and the high-grade gneiss assemblages known as the Mozambique orogenic belt (Kennedy, 1964; Pinna and others, 1993; Moseley, 1993; Shackleton, 1996) farther south. It extends for ~7000 km

*Institut für Geowissenschaften, Universität Mainz, 55099 Mainz, Germany

**Institut für Geochemie, Universität Tübingen, Wilhelmstraße 56, 72074, Tübingen, Germany. Present address: Institut für Mineralogie, Universität München, Theresienstrasse 41, 80333 München, Germany

***Orogenic Processes Group, Department of Geology, University of Leicester, Leicester LE1 7RH, United Kingdom. Present address: Tectonics Special Research Centre, School of Applied Geology, Curtin University of Technology, G.P.O. Box U1987, Perth, Western Australia 6845, Australia

****Orogenic Processes Group, Department of Geology, University of Leicester, Leicester LE1 7RH, United Kingdom

*****Département des Sciences Naturelles, Université de Toliara, Toliara, Madagascar

******Department of Applied Geology, Curtin University of Technology, P.O. Box U1987, Perth, Western Australia 6845, Australia

along the eastern part of Africa from Egypt to Mozambique which makes it one of the largest orogenic belts on the globe. This orogen evolved in Neoproterozoic time (that is, between ~850 and ~550 Ma ago). It is only with the increased use of precise geochronological techniques, coupled with detailed field studies (Stern, 1994; Windley and others, 1994; Shackleton, 1996; Meert and Van der Voo, 1997; Kröner and others, 1999; Collins, Razakamanana, and Windley, 2000), that these Neoproterozoic tectonic events are beginning to be subdivided.

In a tight-fit reconstruction of Gondwana for 200 Ma (Lawver, Gahagan, and Coffin, 1992), Madagascar lies in the heart of the East African orogen with a small fragment of Archean eastern foreland rocks preserved in the northeast of the island (Collins, Razakamanana, and Windley, 2000). In central and northern Madagascar, Collins and others (2000) identified a series of tectonic units. Rocks within each unit share similar tectonic histories, but each unit has a different geological record compared to that of its neighbors. These five tectonic units (fig. 1) are discussed below briefly.

The Antananarivo Block forms the basement of much of Central Madagascar and is dominated by a thick swath of migmatites, orthogneisses, and granites that crop out in a broad north-south band across the island (Besairie, 1968-1971; Windley and others, 1994; fig. 1). To the east of the Antananarivo Block, meta-igneous rocks pass structurally down into paragneiss and orthogneiss with podiform ultrabasic rocks. These rocks, in turn, pass structurally down into amphibolite- and greenschist-facies metapelites that rim a metagranite terrain that crops out on the northeast coast (fig. 1). Rb-Sr (Vachette, 1979) and U-Pb zircon dates (Tucker and others, 1999) indicate that this northeastern granite is Archean (the Archean granite and surrounding metapelites are referred to as the Antongil block after Hottin, 1976; fig. 1).

Structurally overlying and possibly interleaved with rocks of the Antananarivo block are a series of amphibolite-grade metabasic gneisses interlayered with podiform chromitites and intruded by gabbros and granites. These form four elongate north-south belts. From west to east these are the Maevatanana, Andriamena, Alaotra-Beforona, and Androna belts (Besairie, 1968-1971; Hottin, 1976). These four lithologically similar belts are interpreted to form part of the same tectonic unit and are here referred to as the Tsaratanana thrust sheet (fig. 1). In the north of the island an enigmatic series of paragneisses, orthogneisses, granites, quartzites, and schists tectonically overlies and truncates structures in the Antongil block, the Tsaratanana thrust sheet, and the Antananarivo block (Besairie, 1973). The structural trend in this northern region (hereafter referred to as the Bemarivo belt) is oblique to the trend in both the Antananarivo and Antongil blocks with foliation dominantly dipping to the north and striking roughly east-west (fig. 1).

Finally, in the center of the island a series of Proterozoic metasediments and metabasites constitute the Itremo thrust sheet (Cox, Armstrong, and Ashwal, 1998), also known as the "Séries Schisto-Quartzo-Calcaire" (Besairie, 1968-1971) and the "Série Schisto-Quartzo-Dolomitique" (Moine, 1968). These lie in a similar structural position to the Tsaratanana thrust sheet – that is, directly above the Antananarivo block. The boundary between the Itremo thrust sheet and the Antananarivo block is split into two domains, based on kinematic and structural style. West of Antsirabe (fig. 1), the boundary is imbricated and preserves evidence of contractional deformation (top-to-the-east – up-foliation – shear sense). South of Antsirabe, the boundary forms an extensional shear zone (Collins and others, 2000).

This paper is concerned with the Antananarivo block which forms the bulk of central Madagascar, and all samples discussed below are derived from exposures within this block (fig. 2).

Several tectonothermal events have been recognized within Madagascar (Besairie, 1968 to 1971; Hottin, 1976; Windley and others, 1994; Windley and Razakamanana,

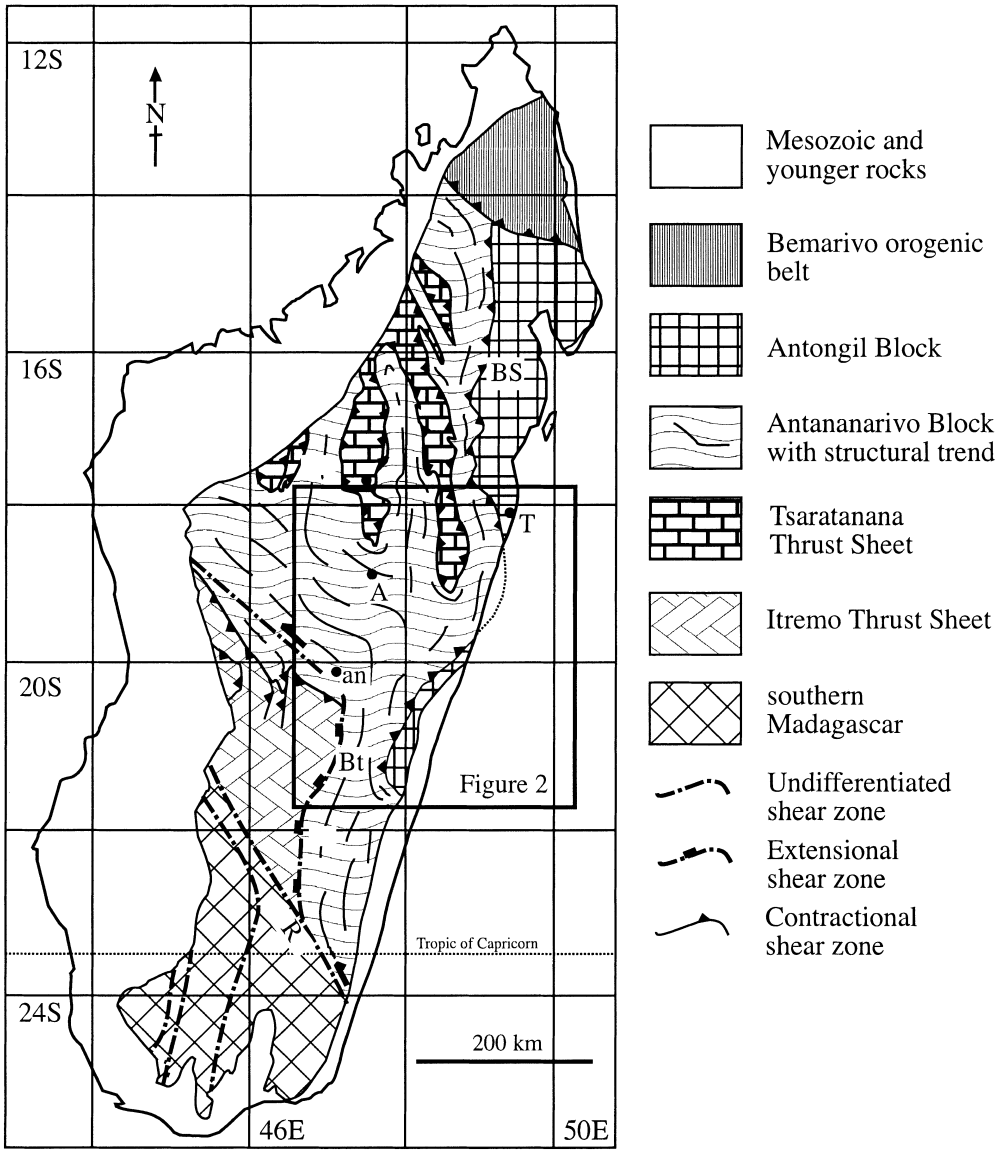

Fig. 1. Simplified geological map showing major tectonic units of the Precambrian in Madagascar (modified from Collins and others, 2000). A = Antananarivo, T = Toamasina, an = Antsirabe. R = Rantosara shear zone; Bt = Betsileo shear zone; BS = Betsimisiraka suture.

1996; Nédélec and others, 1994; Nédélec, Stephens, and Fallick, 1995; Tucker and others, 1997, 1999; Kröner and others, 1999; Collins, Razakamanana, and Windley, 2000). Tucker and others (1997) identified three crust-forming and reworking events from a large database of high precision U-Pb zircon geochronology. These were defined as middle Archean-Paleoproterozoic (2520-2495 Ma), middle Neoproterozoic (790-637 Ma), and late Neoproterozoic-Cambrian (580-520 Ma). The previously unrecognized 790 to 637 Ma event is particularly intriguing as this age bracket spans the period proposed for contractional deformation within central Madagascar (Cox and Armstrong,

Sample	Pb/Pb evaporation age in Ma
Mad 108	517.8±1.0
Mad 63	537.6±1.0
Mad 104	551.0±1
Mad 79	554.4±1.0
Mad 102	554.4±1
M1	589.1±1
Mad 117	719.3±0.4
Mad 50	739.5±0.9
Mad 60	741.2±0.9
Mad 61	742.6±0.9
Mad 107	749.8±0.9
Mad 67	750.0±0.9
Mad 88	758.3±0.9
Mad 80	763.7±0.9
Mad 99	770±18*
Mad 66	774.0±0.9
Mad 62	778.5±0.9
Mad 76	788.8±0.9
Mad 68	789.0±0.9
Mad 74	791.1±0.9
Mad 73	792.2±0.9
Mad 78	801±2*
Mad 64	818±6*
Mad 65	2510±0.3
Mad 103	2514±6*
Mad 69	2528±19*
Mad 89	2550±10*

* = SHRIMP II concordia upper intercept ages

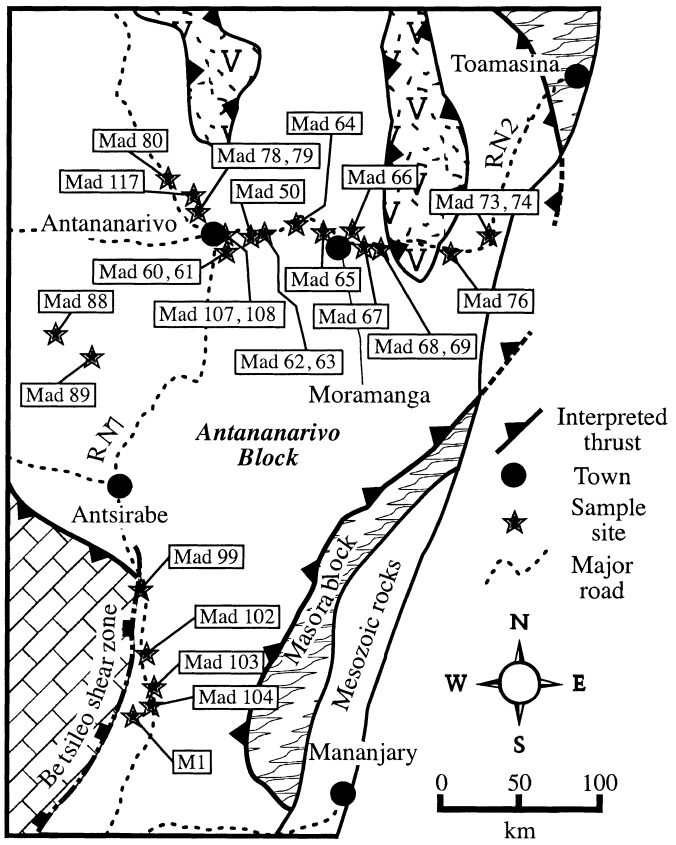

Fig. 2. Geological map of central Madagascar showing major rock units and locations of samples dated in this study.

1997; Nédélec and Paquette, 1997; Cox, Armstrong, and Ashwal, 1998). We present new single zircon geochronological data produced by SHRIMP and Pb-Pb evaporation techniques as well as whole-rock Nd isotopic systematics from central Madagascar. These data indicate that early Neoproterozoic magmatism was much more extensive than previously thought, occurring throughout much of the Antananarivo block. The precise location of the dated samples as well as the main mineral centent are given in table 1.

ANALYTICAL PROCEDURES

Zircons were separated using a Wilfley table, magnetic separator, heavy liquids, and final handpicking. Single zircons were analyzed using the single zircon evaporation method (Kober, 1986, 1987) and the SHRIMP II ion-microprobe of the Perth Consortium, Australia. In addition, we determined the Sm–Nd whole-rock isotopic composition of selected samples to calculate Nd model ages and $\epsilon_{Nd(t)}$ values. The geochemistry of our dated samples is presented in table 2 but will be discussed elsewhere (Brewer and others, in preparation).

Single zircon evaporation.–We used the method developed by Kober (1986) involving repeated evaporation and deposition of Pb from chemically untreated single zircons in a double-filament arrangement (Kober, 1987). Our laboratory procedures as well as

TABLE 1

Sample location and main mineral content

Sample no.	Location	Main minerals*
Mad 50	S18° 53', E47° 43'	Hbl, Bt, Pl, Opx, Qtz
Mad 60	S18° 53.987', E47° 34.250'	Pl, perthitic Kfs, Qtz, Bt
Mad 61	S18° 53.987', E47° 34.250'	Pl, perthitic Kfs, Mc, Qtz, Bt
Mad 62	S18° 53', E47° 43'	perthitic Kfs, Qtz, Pl, Bt
Mad 63	S18° 54', E47° 45'	perthitic Kfs, Qtz, Pl, Hbl, Bt, Ms
Mad 64	S18° 55', E47° 56'	Pl, Bt, Opx, Cpx, Qtz
Mad 65	S18° 57', E48° 16'	Pl, Hbl, Bt, Cpx, Qtz
Mad 66	S18° 55', E48° 25'	Kfs, Pl, Hbl, Bt, Grt, Qtz
Mad 67	S18° 57', E48° 26'	Hbl, Bt, Pl, Kfs, Qtz
Mad 68	S18° 56', E48° 28'	Hbl, bt, Pl, Kfs, Qtz
Mad 69	S18° 58', E48° 34'	Hbl, Bt, Pl, Qtz
Mad 73	S18° 43', E48° 04'	Bt, Pl, Kfs, Mc, Grt, Qtz
Mad 74	S18° 43', E48° 04'	Hbl, Bt, Pl, perthitic Kfs, Mc, Grt, Qtz
Mad 76	S18° 57' E48° 48.5'	Hbl, Bt, Pl, Kfs, Qtz
Mad 78	S18° 47.688', E47° 27.490'	Pl, Kfs, Bt, Qtz, Cpx
Mad 79	S18° 47', E47° 25'	Kfs, Pl, Qtz, Bt
Mad 80	S18° 41.82', E47° 17.25'	Kfs, Pl, Hbl, Bt, Qtz
Mad 88	S19° 21', E46° 45'	Hbl, Bt, Pl, Kfs, Qtz
Mad 89	S19° 40', E46° 55'	Hbl, Pl, Kfs, Qtz
Mad 99	S20° 05.7', E47° 02.2'	Hbl, Pl, Kfs, Qtz
Mad 102	S20° 26.4', E47° 11.6'	Hbl, Bt, Pl, perthitic Kfs, Qtz, relict Cpx
Mad 103	S20° 33', E47° 14'	Hbl, Bt, Pl, Qtz
Mad 104	S20° 37', E47° 12'	Bt, Pl, Kfs, Qtz
Mad 107	S18° 55.0', E47° 33.8'	Kfs, Pl, Qtz, Bt
Mad 108	S18° 55.0', E47° 33.8'	Kfs, Pl, Qtz, Bt
Mad 117	S18° 46.2', E47° 28.8	Pl, perthitic Kfs, Qtz, Hbl, Bt
M-1	S20° 39', E47° 09'	Kfs, Pl, Qtz, Bt, Ms

*Abbreviation of mineral names after Kretz (1983).

comparisons with conventional and ion-microprobe zircon dating are detailed in Kröner and Todt (1988), and Kröner and Hegner (1998). Isotopic measurements were carried out on a Finnigan-MAT 261 mass spectrometer at the Max-Planck-Institut für Chemie in Mainz.

The calculated ages and uncertainties are based on the means of all ratios evaluated and their 2σ mean errors. Mean ages and errors for several zircons from the same sample are presented as weighted means of the entire population. During the course of this study we repeatedly analyzed fragments of large zircon grains from the Palaborwa Carbonatite, South Africa. These zircons, used as an internal standard, are euhedral, colorless to slightly pink, and completely homogeneous when examined under cathodoluminescence. Conventional U-Pb analyses of six separate grain fragments from this sample yielded a $^{207}Pb/^{206}Pb$ age of 2052.2±0.8 Ma (2σ, W. Todt, unpublished data), while the mean $^{207}Pb/^{206}Pb$ ratio for 18 grains, evaporated individually over a period of 12 months, is 0.126634 ± 0.000027 (2σ error of the population), corresponding to an age of 2051.8 ± 0.4 Ma, identical to the U-Pb age. The above error is considered the best estimate for the reproducibility of our evaporation data and corresponds approximately to the 2σ (mean) error reported for individual analyses in this study (table 3). In the case of combined data sets the 2σ (mean) error may become very low, and whenever this

TABLE 2

Chemical composition of samples dated in this study. Major elements in weight %, trace elements in ppm. Rock types based on major oxides after Debon and Le Fort (1982).*

Sample no.	Mad 50	Mad 60	Mad 61	Mad 62	Mad 63	Mad 64	Mad 65	Mad 66	Mad 67	Mad 68	Mad 69	Mad 73	Mad 74
SiO_2	55.88	75.80	76.58	74.63	67.78	53.78	57.97	68.43	69.65	71.80	59.39	71.91	69.68
TiO_2	0.62	0.28	0.25	0.16	0.91	1.15	0.57	0.52	0.53	0.40	0.65	0.50	0.53
Al_2O_3	14.55	12.72	12.49	13.45	14.03	14.49	15.65	13.75	13.43	13.16	16.04	12.91	13.59
$Fe_2O_{3\dagger}$	9.02	1.06	1.33	1.34	4.20	10.92	7.60	4.73	4.45	3.43	7.33	3.14	4.12
MnO	0.15	0.03	0.05	0.02	0.06	0.21	0.13	0.08	0.06	0.05	0.10	0.02	0.05
MgO	6.92	0.33	0.24	0.25	0.90	6.22	5.58	0.18	0.37	0.24	3.31	0.46	0.27
CaO	8.01	1.06	0.80	1.25	2.54	8.53	7.42	2.10	1.87	1.38	5.81	1.47	2.16
Na_2O	2.92	2.78	3.07	3.17	3.18	3.21	3.34	2.78	3.07	2.86	3.70	2.76	2.50
K_2O	1.06	5.49	5.02	5.38	5.38	1.23	1.07	6.69	6.11	6.01	2.71	6.30	6.52
P_2O_5	0.23	0.05	0.04	0.05	0.38	0.21	0.18	0.10	0.10	0.07	0.30	0.17	0.13
LOI	0.45	0.27	0.12	0.40	0.38	0.20	0.51	0.74	0.25	0.22	0.60	0.50	0.31
Total	99.80	99.86	99.98	99.83	99.73	100.14	100.02	100.10	99.88	99.63	99.94	100.14	99.86
Rock type	Quartz syenite	Granite	Granite	Granite	Granite	Quartz diorite	Quartz diorite	Granite	Granite	Granite	Q-monz. diorite	Granite	Granite
Ba	330	1094	895	602	1963	513	452	1168	824	790	1481	942	1008
Rb	20	122	142	209	129	26	12	220	224	242	72	240	225
Sr	463	195	102	145	562	357	489	146	109	99	731	139	146
Mo	1	3	3	2	2	<1	3	2	3	5	1	4	3
Cu	52	4	<1	<1	11	50	38	7	6	7	38	6	8
Zn	90	21	25	26	68	119	77	132	100	86	68	89	72
Ga	19	13	14	18	20	21	20	27	26	25	19	23	24
Sc	27	2	<1	<1	4	27	26	8	4	3	17	<1	2
Pb	14	27	26	35	23	22	7	42	30	40	19	36	36
La	36	49	44	51	117	38	35	76	125	116	22	78	64
Ce	66	77	69	61	260	103	71	153	240	217	47	139	142
Nd	32	29	22	19	90	45	31	67	87	79	27	53	62
Y	27	4	13	<1	48	37	30	60	77	75	20	7	53
Zr	146	194	180	161	493	152	188	680	517	456	162	359	477
Nb	8	8	10	7	31	9	9	26	23	22	5	14	24
V	92	16	16	10	45	172	69	20	20	16	101	22	13
Cr	264	23	17	21	31	144	198	22	18	17	70	18	21
Ni	84	<1	2	2	5	62	61	10	13	11	26	2	7
Th	4	24	25	41	17	<1	<1	13	48	44	3	56	28
U	<1	<1	<1	<1	<1	<1	<1	3	5	4	<1	4	<1

Sample no.	Mad 76	Mad 78	Mad 79	Mad 80	Mad 88	Mad 89	Mad 99	Mad 102	Mad 103	Mad 104	Mad 107	Mad 117	M 1
SiO_2	67.06	68.07	68.27	65.57	71.37	73.44	70.02	57.69	61.92	71.82	68.95	70.81	68.99
TiO_2	0.62	0.46	0.82	0.49	0.41	0.07	0.18	1.85	0.56	0.51	0.44	0.61	0.79
Al_2O_3	13.78	14.68	13.67	16.70	13.97	15.12	15.82	15.24	15.08	13.67	14.96	13.07	14.27
$Fe_2O_{3\dagger}$	5.47	4.23	4.77	3.59	3.00	0.82	2.07	8.93	5.52	2.69	3.36	3.90	3.81
MnO	0.08	0.06	0.06	0.07	0.06	0.03	0.06	0.14	0.08	0.04	0.08	0.07	0.05
MgO	0.30	1.56	0.79	0.96	0.45	0.19	0.38	2.07	4.22	0.62	0.87	0.63	0.76
CaO	2.51	3.47	2.23	2.92	1.44	1.46	1.82	4.73	4.30	1.55	2.36	1.77	1.94
Na_2O	3.15	3.76	3.03	4.69	4.25	6.27	5.40	4.00	3.99	3.27	4.48	3.48	2.60
K_2O	6.37k	3.29	5.46	4.46	4.97	2.81	4.42	4.10	3.73	5.32	3.91	4.98	5.79
P_2O_5	0.14	0.16	0.26	0.21	0.12	0.03	0.07	0.84	0.32	0.13	0.13	0.14	0.21
LOI	0.14	0.37	0.59	0.32	0.18	0.07	0.12	0.04	0.46	0.54	0.11	0.15	0.57
Total	99.61	100.11	99.94	99.98	100.22	100.30	100.37	99.63	100.18	100.17	99.64	99.61	99.77
Rock type	Quartz syenite	Grano-diorite	Granite	Qz mon-zonite	Adam-ellite	Grano-diorite	Qz mon-zonite	Quartz diorite	Qz mon-zodiorite	Granite	Adam-ellite	Granite	Adam-ellite
Ba	1293	1170	1908	1808	1159	1707	1916	3553	1065	1069	1036	983	1463
Rb	190	72	134	73	92	39	104	84	136	348	85	151	254
Sr	166	460	329	546	198	1319	1401	1132	465	223	266	151	243
Mo	5	2	3	2	1	1	1	2	2	1	1	3	<1
Cu	14	21	17	12	2	<1	4	19	4	7	<1	4	10
Zn	102	56	81	45	45	9	42	172	59	58	40	51	37
Ga	26	18	22	18	19	15	18	23	19	21	16	18	20
Sc	8	6	3	6	5	7	8	17	13	6	10	7	<1
Pb	41	28	32	29	21	28	35	30	23	45	24	23	31
La	75	36	163	73	108	8	33	152	73	166	46	60	247
Ce	139	56	330	107	171	<1	15	282	128	278	76	89	490
Nd	58	21	115	39	65	4	19	133	55	74	34	45	149
Y	59	9	57	22	36	4	12	53	31	10	27	99	39
Zr	602	144	935	324	341	56	125	847	246	351	199	352	642
Nb	23	7	37	11	17	4	7	42	10	31	7	20	49
V	21	51	44	38	14	7	14	106	87	28	29	25	36
Cr	25	41	32	37	3	4	3	<1	200	9	4	7	48
Ni	10	11	10	6	5	<1	<1	6	81	6	2	7	11
Th	19	17	14	12	9	1	9	10	27	90	12	15	60
U	5	<1	<1	<1	<1	<1	<1	<1	<1	<1	<1	<1	4

*X-ray fluorescence analyses were carried out at Leicester University, using a Phillips PW 1400 spectrometer and following techniques as detailed in Brewer, Daly, and Åhäll (1998) and Harvey (1989). † = total Fe as Fe_2O_3.

TABLE 3

Pb isotopic data from single grain zircon evaporation

Sample Number	Zircon colour and morphology	Grain #	Mass scans[1]	Evaporation temp. in °C	Mean $^{207}Pb/^{206}Pb$ ratio[2] and 2-σm error	$^{207}Pb/^{206}Pb$ age and 2-σm error
Mad M-1	long-prismatic, ends	1	60	1599	0.059615±46	589.6±1.7
	rounded,	2	104	1600	0.059594±29	588.9±1.0
	light gray	3	105	1602	0.059601±17	589.1±0.6
mean of 3	**grains**	1-3	269		0.059601±16	***589.1±1.0**
	as above	4	65	1598	0.074561±54	1056.7±1.5
Mad 50	long-prismatic, ends	1	96	1599	0.063937±46	739.5±1.5
	well rounded, clear	2	143	1601	0.063929±32	739.3±1.0
		3	115	1599	0.063946±21	739.8±0.7
mean of 3	**grains**	1-3	254		0.063937±19	***739.5±0.9**
	round, irregular	4	79	1610	0.100661±50	1636.3±0.9
	spherical, clear,	5	107	1604	0.058553±37	550.5±1.4
	multifaceted	6	95	1607	0.058542±38	550.1±1.4
Mad 60	short- and long-	1	88	1598	0.063987±60	741.2±2.0
	prismatic, ends	2	121	1601	0.063998±29	741.6±1.0
	slightly rounded,	3	110	1602	0.063974±12	740.8±0.4
	clear	4	66	1600	0.063978±37	740.9±1.2
		5	110	1604	0.063984±22	741.1±0.7
		6	88	1601	0.063991±25	741.3±0.8
mean of 6	**grains**	1-6	583		0.063986±14	***741.2±0.9**
	yellow-br., rounded	7	77	1604	0.745761±44	1057.1±1.2
Mad 61	long-prismatic, ends	1	114	1596	0.064060±31	743.6±1.0
	rounded, clear to	2	75	1600	0.063989±41	741.3±1.3
	light brown	3	99	1599	0.064024±20	742.4±0.7
		4	119	1594	0.064034±18	742.8±0.6
mean of 4	**grains**	1-4	407		0.064031±14	***742.6±0.9**
Mad 62	long-prismatic, idio-	1	66	1613	0.065435±54	788.4±1.7
	morphic, very clear	2	66	1601	0.065449±45	788.8±1.4
		3	66	1608	0.065456±31	789.0±1.0
		4	88	1612	0.065420±13	787.9±0.4
mean of 4	**grains**	1-4	286		0.065439±18	***788.5±0.9**
	as above, ends rd.	5	66	1599	0.072746±69	1006.9±1.9
Mad 63	long-prismatic, ends	1	86	1598	0.058212±42	537.8±1.6
	rounded, very clear	2	96	1600	0.058205±27	537.5±1.0
		3	126	1597	0.058207±33	537.6±1.2
		4	84	1597	0.058207±34	537.6±1.3
		5	85	1600	0.058215±33	537.9±1.2
mean of 5	**grains**	1-5	477		0.058209±15	***537.6±1.0**
Mad 65	long-prismatic, ends	1	66	1600	0.150778±43	2354.8±0.5
	rounded, light gray	2	110	1597	0.150822±44	2355.3±0.5
		3	88	1600	0.150753±34	2354.5±0.4
		4	110	1600	0.150802±25	2355.0±0.3
		5	165	1599	0.150804±20	2355.1±0.2
mean of 5	**grains**	1-5	539		0.150796±14	***2355.0±0.3**
Mad 66	long-prismatic, ends	1	92	1599	0.064995±33	774.2±1.1
	rounded, clear	2	136	1606	0.064978±19	773.6±0.6
		3	101	1602	0.064967±24	773.3±0.8
		4	130	1597	0.065013±16	774.8±0.5
mean of 4	**grains**	1-4	459		0.064989±11	***774.0±0.9**
Mad 67	long-prismatic, ends	1	66	1599	0.064246±46	749.7±1.5
	rounded, clear to	2	110	1599	0.064262±15	750.3±0.5
	light gray	3	110	1601	0.064253±22	750.0±0.7
mean of 3	**grains**	1-3	286		0.064255±15	***750.0±0.9**

TABLE 3
(continued)

Sample Number	Zircon colour and morphology	Grain #	Mass scans[1]	Evaporation temp. in °C	Mean $^{207}Pb/^{206}Pb$ ratio[2] and 2-σm error	$^{207}Pb/^{206}Pb$ age and 2-σm error
Mad 68	long-prismatic, ends	1	83	1599	0.065444±24	788.6±0.8
	rounded, clear to	2	87	1600	0.065467±23	789.4±0.7
	light gray	3	99	1602	0.065453±23	788.9±0.7
mean of 3	**grains**	1-3	269		0.065455±13	***789.0±0.9**
Mad 73	long-prismatic, ends	1	108	1602	0.065546±36	791.9±1.2
	rounded, light	2	81	1605	0.065550±40	792.0±1.3
	yellow-brown	3	83	1599	0.065554±26	792.2±0.8
		4	83	1600	0.065528±17	791.3±0.5
		5	88	1602	0.065595±29	793.5±0.9
		6	121	1603	0.065561±19	792.4±0.6
mean of 6	**grains**	1-6	564		0.065556±12	***792.2±0.9**
Mad 74	long-prismatic, ends	1	88	1607	0.065539±48	791.7±1.5
	slightly rounded,	2	88	1606	0.065508±41	790.7±1.3
	clear	3	110	1599	0.065519±26	791.0±0.8
mean of 3	**grains**	1-3	269		0.065520±19	***791.1±0.9**
Mad 76	long-prismatic, ends	1	77	1612	0.065429±49	788.2±1.6
	rounded, clear to	2	77	1600	0.065479±43	789.8±1.4
	light gray	3	88	1605	0.065450±29	788.8±0.9
		4	88	1608	0.065438±19	788.5±0.6
mean of 4	**grains**	1-4	260		0.065449±20	***788.8±0.9**
Mad 77	long-prismatic, ends	1	95	1602	0.166458±29	2522.3±0.3
	rounded, clear to	2	118	1600	0.166474±25	2522.5±0.2
	light gray	3	103	1599	0.166546±27	2523.2±0.3
		4	77	1598	0.166478±44	2522.5±0.4
		5	99	1607	0.166439±44	2522.2±0.4
mean of 5	**grains**	1-5	492		0.166480±15	***2522.6±0.3**
Mad 78	long-prismatic, ends	1	105	1601	0.065524±26	791.2±0.8
	rounded, clear to	2	120	1600	0.065543±23	791.8±0.7
	light gray	3	117	1604	0.065533±21	791.5±0.7
		4	75	1602	0.065539±38	791.7±1.2
		5	75	1601	0.065491±35	790.2±1.1
		6	125	1603	0.065519±24	791.0±0.8
mean of 6	**grains**	1-6	617		0.065532±11	***791.5±0.9**
	as above ends rd.	7	96	1599	0.165775±69	2515.4±0.7
Mad 79	long-prismatic, ends	1	77	1600	0.058665±37	554.6±1.4
	slightly rounded,	2	66	1599	0.058638±35	553.7±1.3
	clear to light yellow	3	99	1599	0.058651±27	554.7±1.0
		4	110	1600	0.058662±27	554.6±1.0
		5	99	1597	0.058648±27	554.1±1.0
mean of 5	**grains**	1-5	451		0.058657±13	***554.4±1.0**
	as above ends rd.	6	66	1601	0.064285±40	751.0±1.3
		7	77		0.106187±64	1735.0±1.1
Mad 80	long-prismatic, ends	1	96	1600	0.064651±37	763.0±1.2
	rounded, clear	2	77	1597	0.064675±38	763.8±1.2
		3	131	1595	0.064664±22	763.4±0.7
		4	115	1598	0.064696±22	764.5±0.7
mean of 4	**grains**	1-4	419		0.064672±14	***763.7±0.9**
Mad 88	long-prismatic, ends	1	66	1603	0.064521±48	758.8±1.6
	rounded, clear to	2	121	1610	0.064492±26	757.8±0.8
	light yellow	3	110	1606	0.064525±27	758.9±0.9
		4	66	1609	0.064484±29	757.5±0.9
mean of 4	**grains**	1-4	363		0.064506±16	***758.3±0.9**

TABLE 3
(continued)

Sample Number	Zircon colour and morphology	Grain #	Mass scans[1]	Evaporation temp. in °C	Mean $^{207}Pb/^{206}Pb$ ratio[2] and 2-σm error	$^{207}Pb/^{206}Pb$ age and 2-σm error
Mad 89	long-prismatic, ends	1	88	1604	0.169195±64	2549.7±0.6
	slightly rounded,	2	77	1613	0.169143±69	2549.2±0.7
	clear to light gray	3	88	1602	0.169095±47	2548.7±0.5
mean of 3	**grains**	1-3	242		0.169145±35	**2549.2±0.3**
Mad 102	long-prismatic,	1	87	1599	0.058641±34	553.8±1.3
	idiomorphic,	2	53	1604	0.058664±48	554.7±1.8
	very clear	3	103	1603	0.058659±29	554.5±1.1
mean of 3	**grains**	1-3	243		0.058654±20	***554.4±1.0**
	yellowish, ends rd.	4	66	1604	0.061771±68	666.2±2.3
Mad 103	long-prismatic, ends	1	74	1598	0.165655±77	2514.2±0.8
	rounded, clear to	2	93	1599	0.165656±78	2514.2±0.8
	light gray	3	63	1601	0.165666±50	2514.3±0.5
		4	82	1598	0.165734±60	2515.0±0.6
		5	88	1600	0.165645±41	2514.1.2±0.4
		6	99	1606	0.165668±42	2514.3±0.4
mean of 6	**grains**	1-6	499		0.165670±24	***2514.4±0.3**
Mad 104	long-prismatic, ends	1	73	1599	0.058563±29	550.9±1.1
	slightly rounded,	2	88	1600	0.058563±29	550.9±1.1
	light gray	3	87	1599	0.058566±14	551.0±0.5
		4	135	1602	0.058570±14	551.2±0.5
mean of 4	**grains**	1-4	383		0.058566±10	***551.0±1.0**
	long-prism., ends	5	77	1599	0.076904±53	1118.7±1.4
	well rd., light gray	6	86	1606	0.136913±64	2188.5±0.8
Mad 107	long-prismatic, ends	1	110	1600	0.064243±26	749.6±0.8
	slightly rounded,	2	132	1602	0.064256±21	750.1±0.7
	light gray	3	154	1601	0.064227±17	749.1±0.6
		4	143	1602	0.064262±16	750.3±0.5
mean of 4	**grains**	1-4	539		0.064247±10	***749.8±0.9**
Mad 108	long-prismatic, idio-	1	93	1602	0.057686±39	517.9±1.5
	morphic, clear to	2	88	1618	0.057685±42	517.8±1.6
	light yellow	3	78	1608	0.057678±39	517.6±1.5
		4	117	1599	0.057679±19	517.6±0.7
		5	61	1598	0.057698±44	518.3±1.7
mean of 5	**grains**	1-5	437		0.057684±16	***517.8±1.0**
Mad 117	long-prismatic, ends	1	88	1604	0.063317±40	718.9±1.3
	rounded, light brown	2	110	1604	0.063330±27	550.9±1.1
	to light gray	3	132	1602	0.063311±23	718.7±0.8
		4	121	1599	0.063328±23	719.3±0.8
mean of 4	**grains**	1-4	451		0.063328±12	***719.3±0.9**
	as above, ends rd.	5	77	1600	0.074557±44	1056.6±1.2
Mad 136	long-prismatic, ends	1	66	1600	0.190605±23	2747.4±0.2
	rounded, dark red	2	132	1599	0.190484±21	2746.3±0.2
mean of 2	**grains**	1&2	198		0.190525±18	***2746.7±0.2**

[1]Number of $^{207}Pb/^{206}Pb$ ratios evaluated for age assessment. [2]Observed mean ratio corrected for nonradiogenic Pb where necessary. Errors based on uncertainties in counting statistics. *Error based on reproducibility of internal standard.

error was less than the reproducibility of the internal standard, we have used the latter value (that is, an assumed 2σ error of 0.000027).

The analytical data are presented in table 3, and the $^{207}Pb/^{206}Pb$ spectra are shown in histograms that permit visual assessment of the data distribution from which the ages

are derived. The evaporation technique provides only Pb isotopic ratios, and there is no *a priori* way to determine whether a measured $^{207}Pb/^{206}Pb$ ratio reflects a concordant age. Thus, principally, all $^{207}Pb/^{206}Pb$ ages determined by this method are necessarily *minimum* ages. However, many studies have demonstrated that there is a very strong likelihood that these data represent true zircon crystallization ages when (1) the $^{207}Pb/^{206}Pb$ ratio does not change with increasing temperature of evaporation and/or (2) repeated analyses of grains from the same sample at high evaporation temperatures yield the same isotopic ratios within error. Comparative studies by single grain evaporation, conventional U–Pb dating, and ion-microprobe analysis have shown this to be correct (Cocherie and others, 1992; Jaeckel and others, 1997; Kröner and others, 1997a; Karabinos, 1997).

SHRIMP II analysis.–Zircons were handpicked and mounted in epoxy resin together with chips of the Perth Consortium standard CZ 3 (Pidgeon and others, 1994). The mount was then polished, cleaned, and etched in 48 percent HF for about 20 sec. Etching brings out the high-U, metamict parts of zircon in that the surface of the polished mount acquires a distinctly gray hue in reflected light, whereas the undamaged portions remain white. The etched zircons were photographed in reflected and transmitted light to bring out the internal structures and to enable easy location on the mount during SHRIMP analyses. The mount was then repolished to remove the etched surface, cleaned, and gold-coated.

Isotopic analyses were performed on the Perth Consortium SHRIMP II ion microprobe, and instrumental characteristics were outlined by De Laeter and Kennedy (1998). The analytical procedures are detailed in Compston and others (1992), Claoué-Long and others (1995), and Nelson (1997). The 1-sigma error in the ratio $^{206}Pb/^{238}U$ during analysis of all standard zircons during this study was between 1.33 and 1.65 percent. Primary beam intensity was between 2.2 and 2.8 nA, and a Köhler aperture of 100 µm diameter was used, giving a slightly elliptical spot size of about 30 µm. Peak resolution was about 4900 A, enabling clear separation of the ^{208}Pb-peak from the HfO-peak. Sensitivity varied between 20 and 30 cps/ppm Pb. Raw data reduction followed the method described by Nelson (1997). Common-Pb corrections have been applied, assuming that common-Pb is surface-related (Kinny, 1986) and using the isotopic composition of Broken Hill lead. The analytical data are presented in table 4. Errors given on individual analyses are based on counting statistics. They are at the 1-sigma level and include the uncertainty of the standard added in quadrature. Errors for pooled analyses are at 2-sigma or 95 percent confidence. The ages and 2σ errors of intercepts of the best-fit line with concordia were calculated using the ISOPLOT program of Ludwig (1994), adapted for the Apple Macintosh by Nemchi, Pidgeon, and Wilde (1994). These errors were not multiplied with the square root of the MSWD, since the absolute value of the intercept error is strongly model-dependent. Whenever isochron criteria were fulfilled for best-fit lines, the model 1 solution was accepted. For cases of greater scatter of data we applied model 4U, that is, the data were weighted according to their degree of discordancy with respect to the upper concordia intercept (Ludwig, 1994).

Several of the SHRIMP II ages reported below are imprecise, since the ion microprobe is not suited for accurate measurement of $^{207}Pb/^{206}Pb$ ages of relatively young zircons that have low uranium contents. Small differences in radiogenic $^{207}Pb/^{206}Pb$ imply large differences in apparent age, and the uncertainties in measuring small amounts of radiogenic ^{207}Pb due to low count rates and the sensitivity to the common Pb correction combine to make the corrected $^{207}Pb/^{206}Pb$ much more imprecise than the other techniques used in this study. On the other hand, the $^{206}Pb/^{238}U$ ratio can be determined to a precision of 2 to 3 percent on SHRIMP II, and if the effects of post-crystallization Pb-loss are negligible and no inherited radiogenic Pb is present, that is, in the case of concordant analyses, the resulting $^{206}Pb/^{238}U$ age provides the most

TABLE 4

SHRIMP II analytical data for spot analyses of single zircons from high-grade granitoid gneisses from central Madagascar

Samle No.	U ppm	Th ppm	$^{206}Pb/^{204}Pb$	$^{208}Pb/^{206}Pb$	$^{207}Pb/^{206}Pb$	$^{206}Pb/^{238}U$	$^{207}Pb/^{235}U$	$^{206}Pb/^{238}U$ age	$^{207}Pb/^{235}U$ age	$^{207}Pb/^{206}Pb$ age
Mad 64- 1	118	37	929	0.1019± 71	0.0666±32	0.1210±14	1.111± 56	736± 8	759±27	825± 97
Mad 64- 2	84	210	1476	0.8030±138	0.0668±42	0.1106±13	1.019± 68	676± 8	713±34	830±129
Mad 64- 3	65	46	5930	0.2336±114	0.0665±48	0.1188±14	1.089± 81	723± 9	748±39	821±144
Mad 64- 4	204	472	5659	0.6911± 54	0.0664±13	0.1330±15	1.217± 30	805± 9	809±14	819± 43
Mad 64- 5	186	426	4277	0.6991± 62	0.0663±16	0.1228±13	1.122± 32	747± 8	764±15	814± 51
Mad 65- 1	384	57	28297	0.0397± 6	0.1656± 6	0.3907±44	8.919±111	2126±20	2330±11	2514± 7
Mad 65- 2	239	129	13249	0.1436± 13	0.1650± 8	0.3983±45	9.062±120	2161±21	2344±12	2508± 9
Mad 65- 3	569	30	9593	0.0155± 12	0.0632± 8	0.1169±12	1.019± 17	713± 7	714± 9	716± 24
Mad 65- 4	41	84	391	0.6372±275	0.0599±10	0.0898±14	0.742±131	555± 8	564±74	601±339
Mad 65- 5	203	194	6037	0.2833± 20	0.1652±10	0.3860±44	8.793±121	2104±21	2317±12	2510± 10
Mad 65- 6	223	75	10520	0.0898± 16	0.1656±12	0.3254±37	7.428±109	1816±18	2164±13	2513± 13
Mad 69- 1	97	79	11364	0.2214± 23	0.1664±13	0.4578±34	10.503±122	2430±15	2480±11	2522± 13
Mad 69- 2	108	70	5587	0.1797± 24	0.1657±13	0.4366±32	9.978±118	2335±14	2433±11	2515± 14
Mad 69- 3	183	149	10989	0.2211± 17	0.1663± 9	0.4527±29	10.379± 96	2407±13	2469± 9	2521± 10
Mad 70- 1	884	324	694	0.1296± 53	0.0583±22	0.0685± 7	0.551± 22	427± 5	446±15	540± 82
Mad 70- 2	988	296	535	0.1125± 47	0.0586±20	0.0821± 9	0.663± 24	509± 5	517±15	552± 73
Mad 70- 3	692	196	1036	0.1177± 41	0.0586±17	0.0822± 9	0.665± 22	509± 5	518±13	555± 64
Mad 70- 4	1448	2572	95	0.4043±107	0.0579±43	0.0674± 8	0.538± 41	420± 5	437±27	528±156
Mad 74- 1	248	13	78927	0.0311± 32	0.0656±15	0.0884±12	0.799± 22	546± 7	569±13	793± 47
Mad 74- 2	256	164	15076	0.1946± 22	0.0656± 9	0.1255±17	1.136± 23	762±10	770±11	794± 27
Mad 74- 3	319	232	1202	0.2306± 34	0.0663±14	0.1317±18	1.204± 31	798±10	803±15	817± 43
Mad 74- 4	116	56	737	0.1543± 73	0.0661±31	0.1248±18	1.137± 58	758±10	771±27	809± 98
Mad 74- 5	149	100	943	0.2306± 63	0.0657±26	0.1290±18	1.169± 51	782±10	786±24	797± 84
Mad 74- 6	119	61	953	0.1655± 57	0.0656±24	0.1306±18	1.181± 48	791±10	792±22	793± 76
Mad 74- 7	135	74	3065	0.1680± 38	0.0656±16	0.1316±18	1.190± 35	797±10	796±16	793± 50
Mad 74- 8	134	71	2192	0.1656± 49	0.0655±21	0.1146±16	1.034± 37	699± 9	721±18	789± 66
Mad 77- 1	91	43	17241	0.1379± 24	0.1663±14	0.4769±37	10.933±134	2517±11	2517±11	2520± 14
Mad 77- 2	877	111	34483	0.0342± 3	0.1643± 3	0.4522±25	10.244± 66	2405±12	2457± 6	2500± 4
Mad 77- 3	124	78	4545	0.1724± 23	0.1650±12	0.4589±32	10.441±116	2435±14	2475±10	2508± 13
Mad 77- 4	572	516	11236	0.2712± 9	0.1650± 5	0.4439±26	10.096± 70	2368±12	2444± 6	2507± 5

accurate estimate of the age for the grain domain analyzed (Williams and Claesson, 1987).

Sm–Nd whole-rock analysis.–Sm–Nd whole-rock isotopic analyses were carried out in the radiogenic isotope laboratory of the University of Tübingen using a technique described in Hegner, Watter, and Satir (1995) and Kröner and Hegner (1998). Total procedural blanks were <30 pg for Nd and Sm and are not significant for the samples of the present study.

Isotopic ratios were measured in static mode using a MAT 262 mass spectrometer. $^{143}Nd/^{144}Nd$ ratios are normalized to $^{146}Nd/^{144}Nd = 0.7219$, and Sm isotopic ratios to $^{147}Sm/^{152}Sm = 0.56081$. During the course of this study the La Jolla Nd standard yielded $^{143}Nd/^{144}Nd = 0.511853 \pm 7$ (2σ, n=6). Two analyses of the rock standard BCR-1 are included in table 3. Within-run precision (2σ mean) for Nd is $\leq 10^{-5}$. The external precision inferred from a large number of analyses is about 1.2×10^{-5} (2 s.d.) for Nd.

The Nd isotopic data are summarized in table 5. The $\epsilon_{Nd(t)}$ values have been calculated for the zircon age determined for each sample, based on the parameters of DePaolo (1981). The Nd model ages were calculated using the two-stage model of Liew and Hofmann (1988). We interpret the Nd model ages in terms of mean crustal residence ages (Arndt and Goldstein, 1987).

SAMPLE DESCRIPTION, ZIRCON MORPHOLOGY, AGES, AND ND SYSTEMATICS

Most of our samples were collected around the capital city of Antananarivo (in short, "Tana") and along the National Road RN2 from Tana to the east coast (fig. 2).

TABLE 5

Sm-Nd isotope data for high-grade gneisses from Madagascar

Sample (Mad)	Zircon age (Ma)	Sm	Nd	$^{147}Sm/^{144}Nd$	$^{143}Nd/^{144}Nd$ *	$\varepsilon_{Nd(t)}$	T_{DM} (Ga)
50	740	5.012	26.64	0.1127	0.511450	-15.2	2.55
62	789	1.358	10.65	0.07708	0.511174	-16.5	2.69
64	818	6.367	30.62	0.1257	0.511604	-12.7	2.42
68	789	6.768	35.70	0.1146	0.511689	-10.2	2.20
73	793	3.419	20.53	0.1007	0.511313	-16.2	2.66
74	791	5.747	25.98	0.1337	0.511573	-14.4	2.53
76	789	4.359	15.99	0.1648	0.511725	-14.6	2.54

*$^{143}Nd/^{144}Nd$: $<10^{-5}$ ($2\sigma_m$, within-run error), external precision $<1.2 \times 10^{-5}$ (2σ).

Several samples come from large quarries around Tana where massive charnockites and enderbites are exposed, showing various stages of retrogression into foliated, granitic biotite-potassium feldspar gneisses (fig. 3). These features are remarkably similar to those seen in the charnockite terrains of Sri Lanka (Baur and others, 1991; Kröner, Jaeckel, and Williams, 1994). Prograde *in-situ* charnockitization, exemplified by blotches and streaks of dark gray-brown charnockite and developed in foliated granite-gneiss in Sri Lanka and southern India (Baur and others, 1991; Newton, 1992) were also observed in the quarry at Ambatomaro near Tana. The relationships demonstrate that the charnockites of central Madagascar were not formed due to intrusion of dry granitic melts at lower crustal levels but resulted from transformation of granitoid gneisses into hypersthene-

Fig. 3. Quarry wall near Antananarivo (disused Carrillion quarry) showing charnockitic gneiss (dark, sample Mad 60) and effect of retrogression leaving a light gray biotite gneiss (sample Mad 61).

bearing assemblages, probably by processes of CO_2-rich fluid infiltration, as previously suggested for similar rocks in southern India and Sri Lanka (Newton, 1992; Newton, Smith, and Windley, 1980; Baur and others, 1991; Milisenda, Pohl, and Hoffmann, 1991).

Below we present and discuss new zircon ages and whole-rock Nd systematics for granitoid orthogneisses and granites of the Antananarivo block (fig. 2), beginning with the area around Tana and moving east to Moramanga, where granulite-facies rocks constitute an appreciable part of the outcrop. We then report data from the area farther east along the RN2 to Toamasina, passing through a region rich in paragneisses where direct evidence for granulite-facies metamorphism is rare, either because of extensive retrogression or lower peak metamorphic conditions. Finally, we report ages from the region south of Tana toward Ambositra and Faratsiho. The chemical characterization of the dated samples (table 2) is after Debon and Lefort (1982).

Granulites and Granites around Tana

Sample Mad 50 of gray-brown, "greasy" enderbitic gneiss is from a blasted roadcut along the RN2 about 21 km due east of Tana (table 1; fig. 2). The chemical data (table 2) classify this rock as a quartz syenite. The zircon population consists predominantly of clear, long-prismatic grains with well-rounded terminations, typical of granitoid rocks that experienced high-grade metamorphism (Silver, 1969; Kröner, Jaeckel, and Williams, 1994). However, there are also rare oval grains with irregular surfaces as well as near-spherical, multifaceted grains typical of metamorphic growth (Kröner, Jaeckel, and Williams, 1994; Jaeckel and others, 1997; Kröner and others, 1998). Three grains were evaporated and yielded identical $^{207}Pb/^{206}Pb$ ratios that combine to a mean age of 739.5 ± 0.9 Ma (table 3; fig. 4A) that we interpret as the time of emplacement of the original quartz syenite protolith from which the enderbitic gneiss was derived. One grain of the round, irregular morphology produced a much older age of 1636.3 ± 0.9 Ma (table 3; fig. 4B) that is interpreted as a xenocryst inherited from the crustal source from which the quartz syenite was derived by melting. Lastly, three of the spherical, multifaceted, metamorphic grains were evaporated together in two separate experiments (because of their small size of ~60 to 80 μm) and yielded identical $^{207}Pb/^{206}Pb$ ratios that yielded a mean age of 550.1 ± 1.4 Ma (table 3; fig. 4C).

Results from whole-rock analysis of sample Mad 50 for Sm and Nd isotopes are presented in table 5. We realize that care must be taken in the use of Nd isotopic systematics for genetic interpretations of rocks that have experienced a high-grade metamorphic history (Moorbath,Whitehouse, and Kamber, 1997). On the other hand, it has been demonstrated that the rare earth elements remain relatively unchanged during high-grade metamorphism (Jahn and Zhang, 1984; Whitehouse, 1989; Condie and others, 1993). Therefore, as long as the Nd isotopic data come from the same sample from which the zircons were dated and are reasonably consistent with the zircon age, we are confident that the Nd isotopic systematics have not been disturbed significantly during post-crystallization events, and that the $\epsilon_{Nd(t)}$ values and Nd mean crustal residence ages provide a reasonable estimate of the source characteristics of the samples under investigation. The $\epsilon_{Nd(t)}$ value for sample Mad 50 with an emplacement age of ~740 Ma is -15.2, while the mean crustal residence age, based on the two-stage model of Liew and Hofmann (1988), is 2.55 Ga. This result suggests an Archean crustal source for the gneiss protolith.

The zircons of this sample and the Nd whole-rock systematics enable us to reconstruct a simplified evolutionary history for sample Mad 50 as follows: (1) The original quartz syenite was derived from a crustal source that contained Paleoproterozoic material and whose mean crustal residence age is 2.42 Ga. (2) Melting of this source at ~740 Ma produced a quartz syenite that subsequently (3) became modified into an

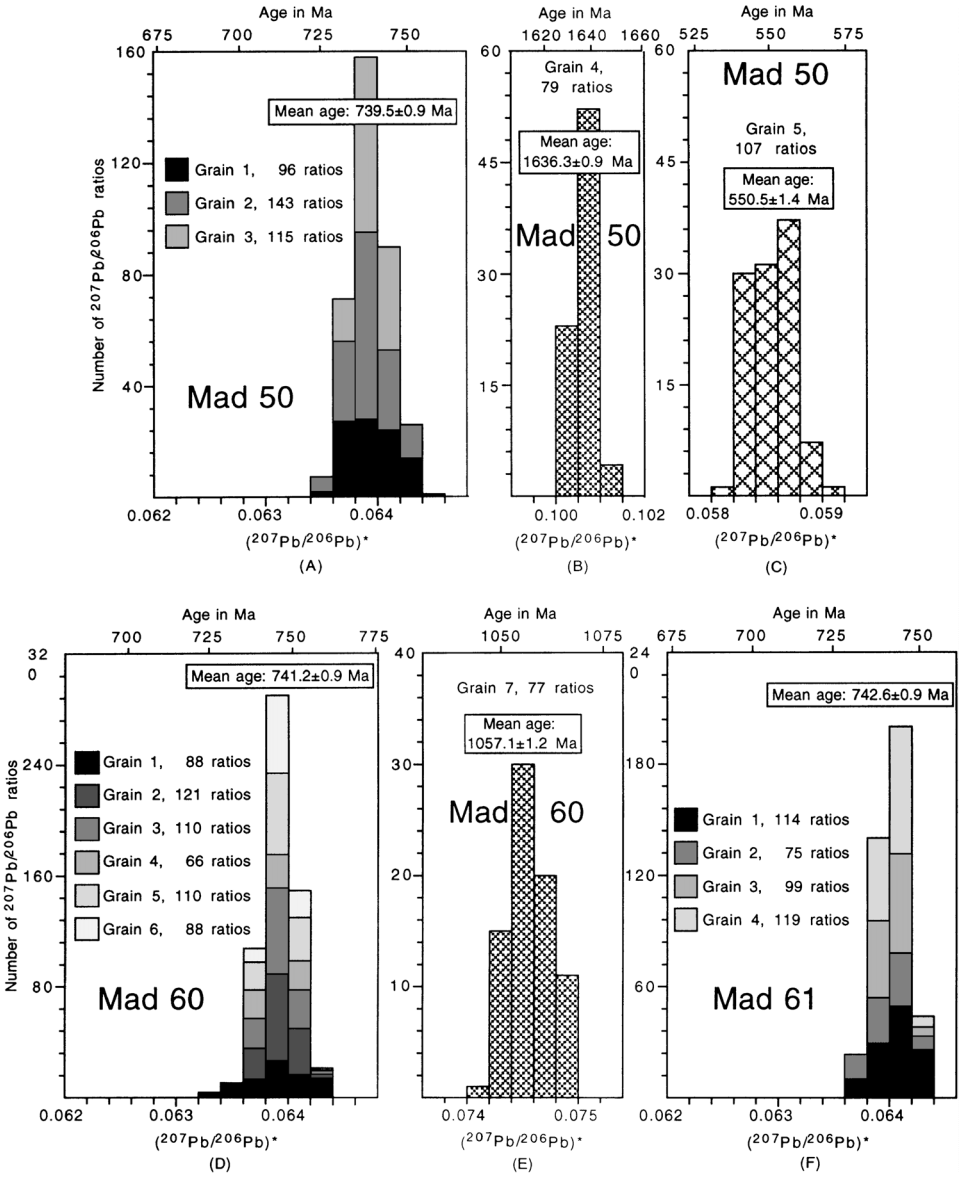

Fig. 4. Histograms showing distribution of radiogenic lead isotope ratios derived from evaporation of single zircons from high-grade gneisses in the area around Antananarivo, central Madagascar. (A) Spectrum for 3 igneous grains from charnockitic gneiss sample Mad 50, integrated from 254 ratios; (B) xenocrystic grain from same sample; (C) round, multifaceted, metamorphic grain from same sample; (D) spectrum for 6 grains from coarse-grained charnockite sample Mad 60, integrated from 583 ratios; (E) spectrum for xenocrystic grain from same sample; (F) spectrum for 3 igneous grains from retrogressed charnockite (now granitic gneiss) sample Mad 61, integrated from 407 ratios.

orthogneiss, possibly during the same event that finally transformed this rock into a enderbitic gneiss during granulite-facies metamorphism at ~550 Ma, as revealed by the age of the metamorphic zircons. The metamorphic event at ~550 Ma is consistent with other data for high-grade rocks from Madagascar ranging from ~560 to 545 Ma (for summary see Kröner, Braun, and Jaeckel, 1996).

Sample Mad 60 was collected in a large abandoned quarry southeast of Tana, known locally as the Carillion quarry (table 1; fig. 2), where charnockitic gneiss of granitic composition (table 3) exhibits spectacular examples of extensive retrogression into a light gray biotite gneiss (fig. 3), similar to examples described from Sri Lanka by Baur and others (1991). Our sample was taken from a coarse charnockite exposed in the lower part of the quarry. The zircons are amost exclusively clear, short- and long-prismatic, and the ends are only slightly rounded. Six grains were evaporated individually and produced a mean $^{207}Pb/^{206}Pb$ age of 741.2±0.9 Ma (table 3; fig. 4D) which we consider to reflect the time of emplacement of the gneiss protolith. One yellow-brown zircon with distinctly rounded terminations yielded a much higher age of 1057.1±1.2 Ma (fig. 4E), and, as in sample Mad 50, we interpret this as a xenocryst inherited from the source region of the granite.

Sample Mad 61 was collected in the same quarry about 15 m above Mad 60 (table 1; fig. 2) and is a light gray, retrogressed charnockitic gneiss of granitic composition (table 2), now a biotite granite gneiss, which contains dark patches of charnockite and which is derived from the same granite as sample Mad 60. The zircons are exclusively clear, long-prismatic and have distinctly rounded terminations. Evaporation of four grains produced consistent $^{207}Pb/^{206}Pb$ ratios that combine to a mean age of 742.6±0.9 Ma (table 3; fig. 4F), indistinguishable from the age for Mad 60 and also interpreted to represent the time of emplacement of the gneiss protolith.

The results for samples Mad 60 and 61 demonstrate that charnockitization and subsequent retrogression apparently had no discernible effect on the original $^{207}Pb/^{206}Pb$ ratios in the magmatic zircons, or at least that such effects were not recognized by the evaporation technique.

The next two samples Mad 107 and 108 come from the large Ambatomaro quarry in Tana, where charnockitic gneiss and its retrogressed equivalents are exposed (table 1; fig. 2). Sample Mad 107, of adamellitic composition (table 2), is from a retrogressed portion of the charnockitic gneiss, whereas Mad 108 was collected from a granite dike truncating both the charnockite and retrogressed granite gneiss and clearly post-metamorphic and post-tectonic in nature. The zircons of Mad 107 are clear to pale yellow and long-prismatic with well rounded terminations. Four grains were evaporated and yielded a combined mean $^{207}Pb/^{206}Pb$ age of 749.8±0.9 Ma (table 3; fig. 5A) which we interpret to reflect the time of emplacement of the charnockitic gneiss precursor.

The zircons of sample Mad 108 are pale yellow to clear, long-prismatic, and perfectly euhedral without cores. Five grains were evaporated and yielded virtually identical $^{207}Pb/^{206}Pb$ ratios that yield a mean age of 517.8±1.0 Ma (table 3; fig. 5E). We interpret this age to reflect the time of granite dike emplacement, and this sets a younger age limit for both the penetrative deformation in the basement rocks and the metamorphism.

Sample Mad 78, a massive, seemingly unfoliated charnockite, was taken from a small quarry at Ivato near Antananarivo International Airport (table 1; fig. 2). This rock is of granodioritic composition (table 2), and the zircons are clear to light gray, long-prismatic and have well rounded terminations. Four grains were analyzed on SHRIMP II (table 4), and two analyses are concordant with a mean $^{206}Pb/^{238}U$ age of 801±2 Ma (fig. 6), while two grains are significantly discordant but can be fitted on a chord through the origin together with the concordant samples. The concordia intercept age of this chord is 791±40 Ma (fig. 6). Evaporation of six grains produced identical $^{207}Pb/^{206}Pb$ ratios that combine to a mean age of 791.5±0.9 Ma (table 3; fig. 6, inset A), identical to the SHRIMP U-Pb concordia intercept age but slightly younger than the concordant ages. We suggest that the evaporated zircons lost a small proportion of their radiogenic lead during high-grade metamorphism, similar to zircons from charnockites in Sri Lanka (Kröner, Jaeckel, and Williams, 1994), and the evaporation age is therefore

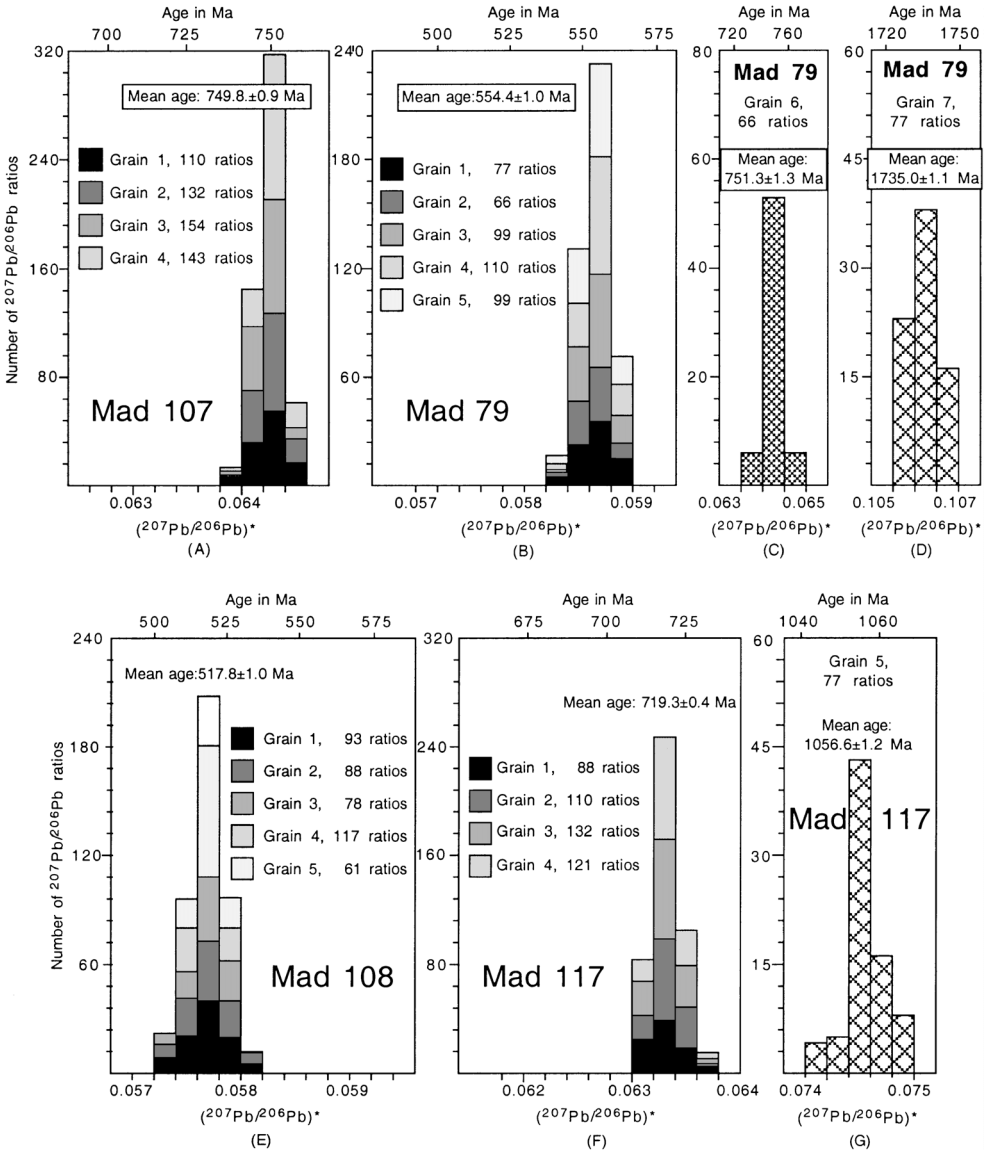

Fig. 5. Histograms showing distribution of radiogenic lead isotope ratios derived from evaporation of single zircons from high-grade gneisses in the area around Antananarivo, central Madagascar. (A) Spectrum for 4 igneous grains from retrogressed charnockitic gneiss sample Mad 107, integrated from 539 ratios; (B) spectrum for 5 igneous grains from weakly foliated granite sample Mad 79, retrogressed from charnockite, integrated from 451; (C, D) spectra for zircon xenocrysts from same sample; (E) spectrum for 5 grains from granitic dike sample Mad 108, integrated from 437 ratios; (F) spectrum for 4 igneous grains from granitic gneiss sample Mad 117, integrated from 451 ratios; (G) spectrum for xenocrystic grain from same sample.

too young. We consider the age of 801±2 Ma to approximate most closely the time of emplacement of the original granodiorite from which the charnockite was derived.

One additional grain, identical in morphology to those above, yielded a much higher evaporation age of 2525.4±0.7 Ma (table 3; fig. 6, inset B) and, in analogy to samples Mad 50 and 60, is interpreted as an inherited xenocryst. This grain demonstrates

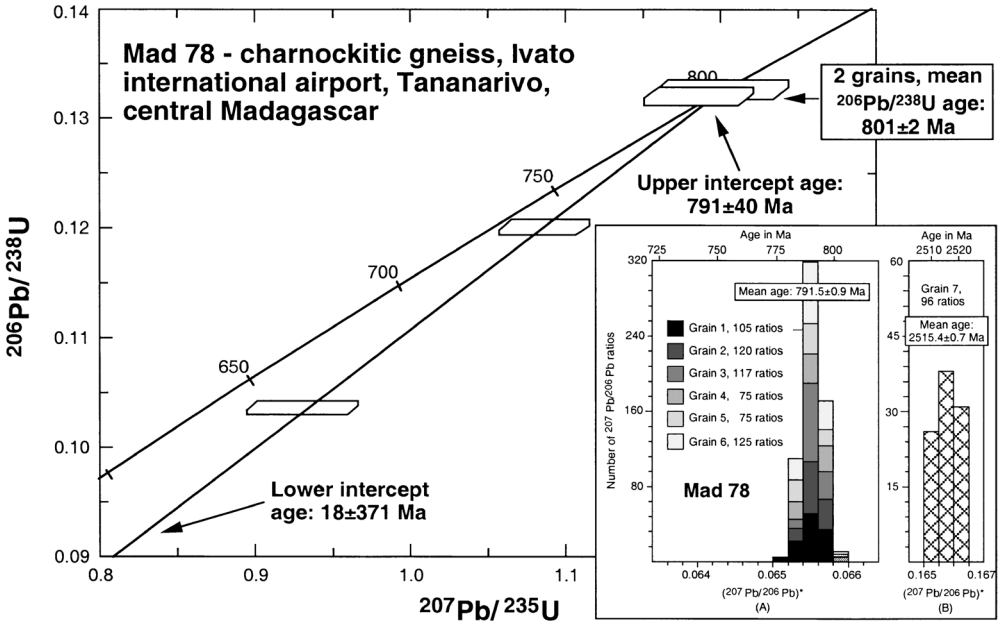

Fig. 6. Concordia diagram showing analytical data for SHRIMP II analyses of zircons from charnockitic gneiss sample Mad 78. Data boxes for each analysis are defined by standard errors in $^{207}Pb/^{235}U$, $^{206}Pb/^{238}U$, and $^{207}Pb/^{206}Pb$. Inset shows histograms with distribution of radiogenic lead isotope ratios derived from evaporation of single zircons from same sample; (A) spectrum for six grains, integrated from 617 ratios; (B) xenocrystic grain from same sample.

that late Archean material is present in the deep crust of central Madagascar, a fact also supported by the whole-rock Nd isotopic systematics.

Sample Mad 79 was collected from a small blasted section a short distance northwest of sample Mad 78 (table 1; fig. 2) and is a weakly foliated granite (table 2) with pods of dark, gray-green charnockite, probably the remains of extensive retrogression from high-grade conditions. The zircons are clear to light yellow, long-prismatic, and slightly rounded at their terminations. Five grains were evaporated and produced consistent $^{207}Pb/^{206}Pb$ ratios that combine to a mean age of 554.4±1.0 Ma (table 3; fig. 5B). We interpret this to be the emplacement age of the granite before it was charnockitized and subsequently retrogressed. This age implies that the peak of granulite-facies metamorphism in the Tana region occurred after ~554 Ma, consistent with the age of 550 Ma obtained for metamorphic zircons in sample Mad 50.

Two additional grains with well rounded ends yielded substantially higher ages of 751.0±1.3 and 1735.0±1.1 Ma respectively (table 3; fig. 5C, D), and we interpret these as xenocrysts inherited from the source material of the original granite.

Sample Mad 117 is a gray biotite gneiss (table 1), derived from a granitic protolith (table 2) and was collected about three km north of Antananarivo International Airport (fig. 2). This gneiss is from the Antananarivo block, only a few kilometers south of the Tsaratanana thrust sheet. The zircons are light yellow-brown to light gray, long-prismatic with slight to well rounded terminations. Evaporation of four grains produced identical isotopic ratios with a mean $^{207}Pb/^{206}Pb$ age of 719.3±0.4 Ma, while one grain was significantly older at 1056.6±1.2 Ma and is interpreted as a xenocryst (table 3; fig. 5F, G). We consider the age of 719 Ma to represent the time of emplacement of the granitic gneiss precursor, whereas the xenocryst of this sample supports the conclusion that some

older crustal material of Kibaran age (broadly equivalent to Grenvillian in North America) was involved in the generation of this rock. Kibaran-age crust may still be present in the deeper crust of central Madagascar today, as indicated by the xenocryst in sample Mad 104 discussed below.

Some 35 km north-northwest of Tana along *Route Nationale* (RN) 4 there is a large, abandoned quarry exposing a sheared contact between charnockite and its retrogressed granite-gneiss equivalent. We collected sample Mad 80 from partly retrogressed charnockitic gneiss (table 1; fig. 2) of quartz monzonitic composition (table 3). The zircons are clear, and their morphology is identical to that in previous charnockite samples (that is, long-prismatic with rounded terminations). Evaporation of four grains yielded a mean $^{207}Pb/^{206}Pb$ age of 763.7±0.9 Ma (table 3; fig. 7A) which we interpret as reflecting the age of emplacement of the original granite from which the charnockitic gneiss was derived.

A large, near-circular granite pluton known as Carion granite (Besairie, 1968-1971; Vachette and Hottin, 1974) is exposed in an abandoned quarry on RN2, 19 km due east of Tana (table 1; fig. 2). This coarse-grained, pink, undeformed porphyritic granite contains numerous xenoliths of dark gray-brown charnockites in various stages of retrogression. We collected sample Mad 62 from one of these charnockite inclusions (table 2). The zircons are almost exclusively clear and long-prismatic, with slightly rounded terminations. Evaporation of four grains produced a mean $^{207}Pb/^{206}Pb$ age of 788.5±0.9 Ma (table 3; fig. 7B) which is considered to date the time of emplacement of the granite from which the charnockite xenolith was ultimately derived. One additional grain with somewhat more rounded ends was significantly older at 1006.9±1.9 Ma and is interpreted as a xenocryst (fig. 7C).

The $\epsilon_{Nd(t)}$ value for sample Mad 62 with an emplacement age of ~789 Ma is -16.5, while the mean crustal residence age, based on a depleted mantle (DM) two-stage model, is 2.69 Ga (table 5). As in sample Mad 50, this result suggests an Archean crustal source for the charnockite protolith.

The zircon ages of samples Mad 50, 60, 61 are similar at 739 to 743 Ma, whilst charnockite sample Mad 62 is some 50 Ma older at ~790 Ma, and charnockite sample Mad 78 is older still at 801 Ma. These results confirm and extend the data set of Tucker and others (1997, 1999) and Handke, Tucker, and Ashwal (1999) who have previously recognized a major event of granitoid magmatism at 775 to 790 Ma in central Madagascar.

We investigated sample Mad 63 of the unfoliated and post-granulite Carion granite exposed in a roadcut along the RN2 east of Tana (table 1; fig. 2). Vachette and Hottin (1974) obtained Rb-Sr whole-rock isochron ages of 682±26 and 527±18 Ma respectively for two granite lithofacies of this pluton. The zircons are uniformly clear, long-prismatic and have slightly rounded terminations. Five isotopically identical grains yielded a mean $^{207}Pb/^{206}Pb$ age of 537.6±1.0 Ma (table 3; fig. 7D) that we interpret as reflecting the time of emplacement of the granite. This age provides a minimum age limit for both Pan-African deformation and metamorphism in central Madagascar.

East of the Carion granite, the rocks along RN2 consist of well foliated charnockitic and enderbitic gneisses that are locally retrogressed to biotite or hornblende granite gneiss. Sample Mad 64 is a dark enderbitic gneiss of quartz dioritic composition (table 2), collected at a roadcut (table 1; fig. 2) and displaying isoclinal folding. The zircons are clear, long-prismatic, lath like, with well-rounded terminations and no visible cores. Five grains were analyzed on SHRIMP II, and the results are listed in table 4 and displayed in figure 8A. One grain is concordant and has a $^{206}Pb/^{238}U$ age of 805±9 Ma while the other grains are variably discordant but can be fitted to a chord through the origin and the concordant point, providing a concordia intercept age of 818±6 Ma. This is interpreted as reflecting the time of emplacement of the original quartz diorite from which the enderbitic gneiss was derived.

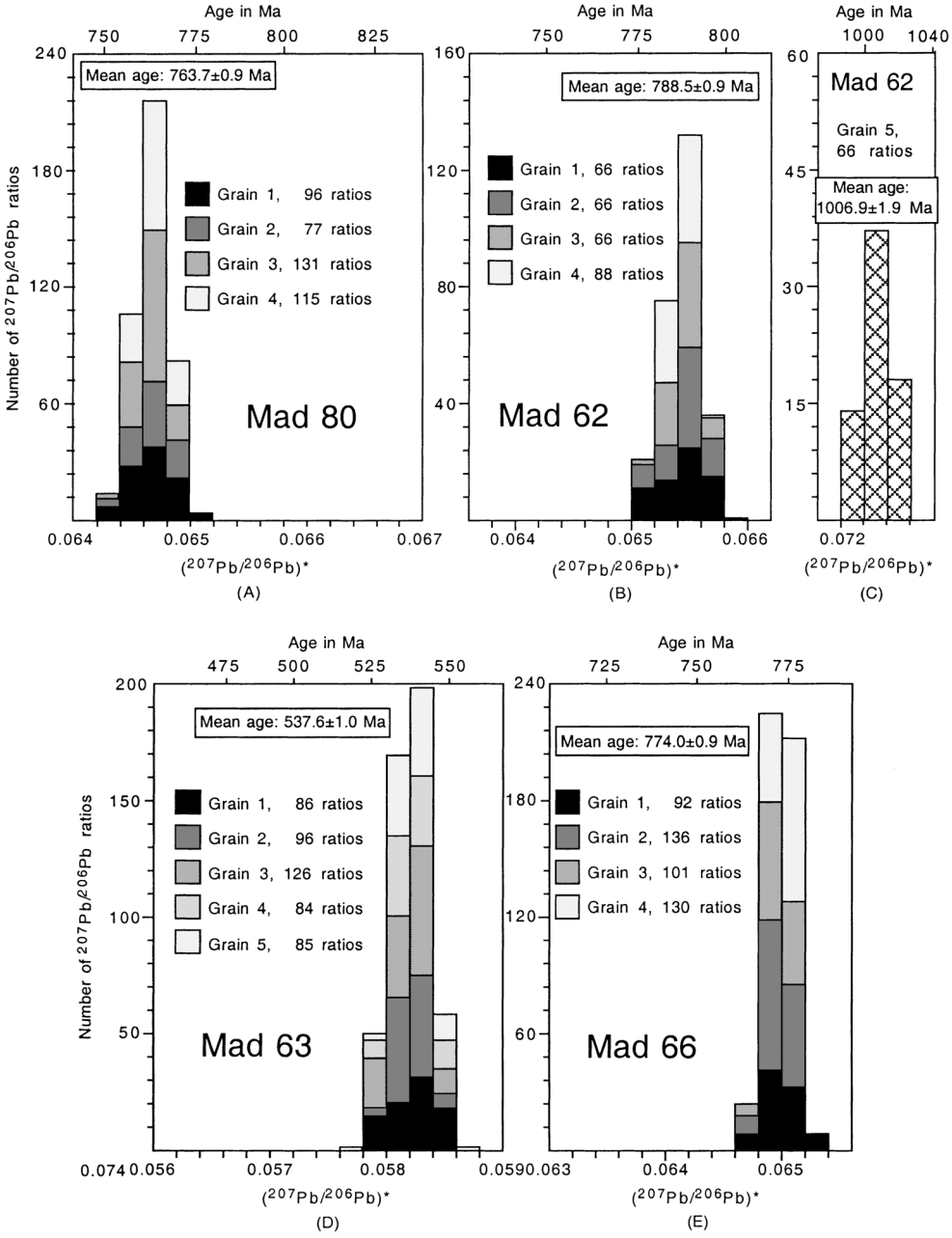

Fig. 7. Histograms showing distribution of radiogenic lead isotope ratios derived from evaporation of single zircons from high-grade gneisses and granites from the area north and east of Antananarivo, central Madagascar. (A) Spectrum for 4 igneous grains from partly retrogressed charnockitic gneiss sample Mad 80, integrated from 419 ratios; (b) spectrum for four grains from pink, coarse-grained, almost undeformed granite sample Mad 62, integrated from 286 ratios; (C) spectrum for xenocrystic grain from same sample; (D) spectrum for 5 grains from Carion granite sample Mad 63, integrated from 477 ratios; (E) spectrum for 4 igneous grains from biotite granite-gneiss sample Mad 66, integrated from 459 ratios.

The $\epsilon_{Nd(t)}$ value in whole-rock sample Mad 64 for an emplacement age of 818 Ma is -12.7, and the mean crustal residence age is 2.42 Ga (table 5). As in the previous samples, derivation from ancient crustal material is the most plausible explanation.

Sample Mad 65 is a well foliated enderbitic gneiss of quartz dioritic composition (table 3), exposed in a quarried river pavement at Moramanga (table 1; fig. 2). The zircons are light gray, long-prismatic with rounded terminations. Six grains were analyzed on SHRIMP II, and the results are quite variable (table 4). The four oldest zircons are all discordant but can be fitted to a chord (MSWD = 0.37) intersecting Concordia at 2508±13 Ma (fig. 8B). The two remaining grains (Mad 65-3 and 65-4) are concordant with $^{206}Pb/^{238}U$ ages of 713±7 and 555±8 Ma respectively (not shown on diagrams). Five grains were evaporated and yielded uniform $^{207}Pb/^{206}Pb$ ratios that combine to a mean age of 2510±0.3 Ma (table 3; fig. 8B, inset). We interpret the array of age data as follows: The age of ~2510 Ma is considered to reflect the time of emplacement of the quartz diorite that was the enderbite precursor. This is supported by nine of the grains analyzed by two different methods. The concordant grain at 713 Ma probably represents new zircon growth during a major thermal event related to the emplacement of voluminous granitoid plutons from which most of the charnockitic-enderbitic gneisses in central Madagascar were derived. The concordant grain at 555 Ma probably grew during high-grade metamorphism that transformed the dioritic gneiss into an enderbite. Alternatively, the enderbite precursor was emplaced at 713 Ma and represents a remelt of ~2510 Ma crustal material, and in this case the Archean zircons are all xenocrysts. We consider this unlikely, however, in view of the abundance of the ancient zircon population and the paucity of ~713 Ma grains.

GRANITOID GNEISSES ALONG RN2 FROM MORAMANGA TO THE EAST COAST

Our next sample, Mad 66, is a strongly foliated, coarse granitic augen-gneiss (table 2) collected from a ductile shear zone in the Sahatany River at a graphite mine at Andasifahatelo (table 1; fig. 2). This rock is most likely retrogressed from granulite-facies to amphibolite-facies during ductile shearing. The zircons are clear, long-prismatic with rounded terminations, a clear indication that they experienced high-grade metamorphism. Four grains were evaporated, and their identical $^{207}Pb/^{206}Pb$ ratios combine to a mean age of 774.0±0.9 Ma (table 3; fig. 7E) that we interpret as reflecting the time of emplacement of the original porphyritic granite from which the augen-gneiss was derived.

Sample Mad 67 was collected in a quarry next to RN2 (table 1; fig. 2) and is a strongly foliated granitic augen-gneiss (table 3) similar to Mad 66. The zircons are clear to light gray, long-prismatic with rounded terminations. Three grains were evaporated and yielded a combined mean age of 750.0±0.9 Ma (table 3; fig. 9A). We interpret this age as representing the time of emplacement of the original porphyritic granite from which this gneiss was derived.

Sample Mad 68 represents a well foliated reddish green, coarse grained, amphibolite facies, biotite bearing, granitic augen gneiss collected at a river outcrop (table 1; fig. 2). The zircons are clear to light gray, long-prismatic with rounded terminations. Three grains were evaporated and yielded a mean $^{207}Pb/^{206}Pb$ age of 789.0±0.9 Ma (table 3; fig. 9B). In analogy with previous samples, we interpret this to represent the time of emplacement of the porphyritic granite from which the augen-gneiss is derived. The $\epsilon_{Nd(t)}$ value in whole-rock sample Mad 68 for an emplacement age of 789 Ma is -10.2, and the mean crustal residence age is 2.20 Ga (table 5). Here again, an old crustal source is indicated for the gneiss protolith, but some minor mantle contribution may also have been involved in the generation of the parent granite.

Sample Mad 69 is a fine-grained biotite-hornblende orthogneiss, derived from a quartz monzodiorite (table 2) and collected from a river outcrop (table 1; fig. 2). This rock is similar in field appearance to the orthogneisses exposed in the "Arenas" or Kadugannawa Complex of central Sri Lanka (Kröner, Cooray, and Vitanage, 1991). The zircons

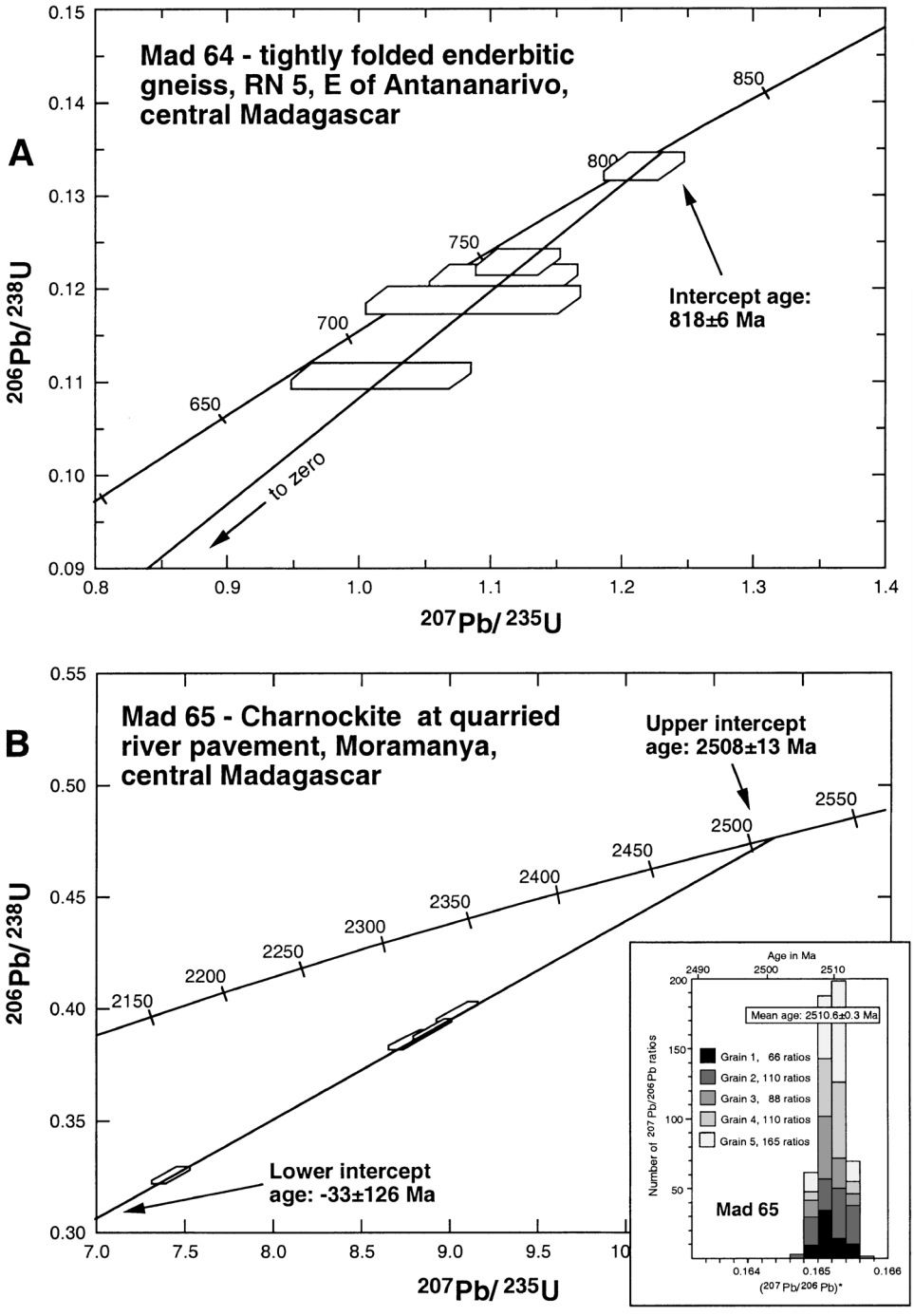
A
Mad 64 - tightly folded enderbitic gneiss, RN 5, E of Antananarivo, central Madagascar
Intercept age: 818±6 Ma
to zero
650
700
750
800
850
206Pb/238U
207Pb/235U
B
Mad 65 - Charnockite at quarried river pavement, Moramanya, central Madagascar
Upper intercept age: 2508±13 Ma
Lower intercept age: -33±126 Ma
2150
2200
2250
2300
2350
2400
2450
2500
2550
Age in Ma
Mean age: 2510.6±0.3 Ma
Grain 1, 66 ratios
Grain 2, 110 ratios
Grain 3, 88 ratios
Grain 4, 110 ratios
Grain 5, 165 ratios
Mad 65
Number of 207Pb/206Pb ratios
(207Pb/206Pb)*

Fig. 8

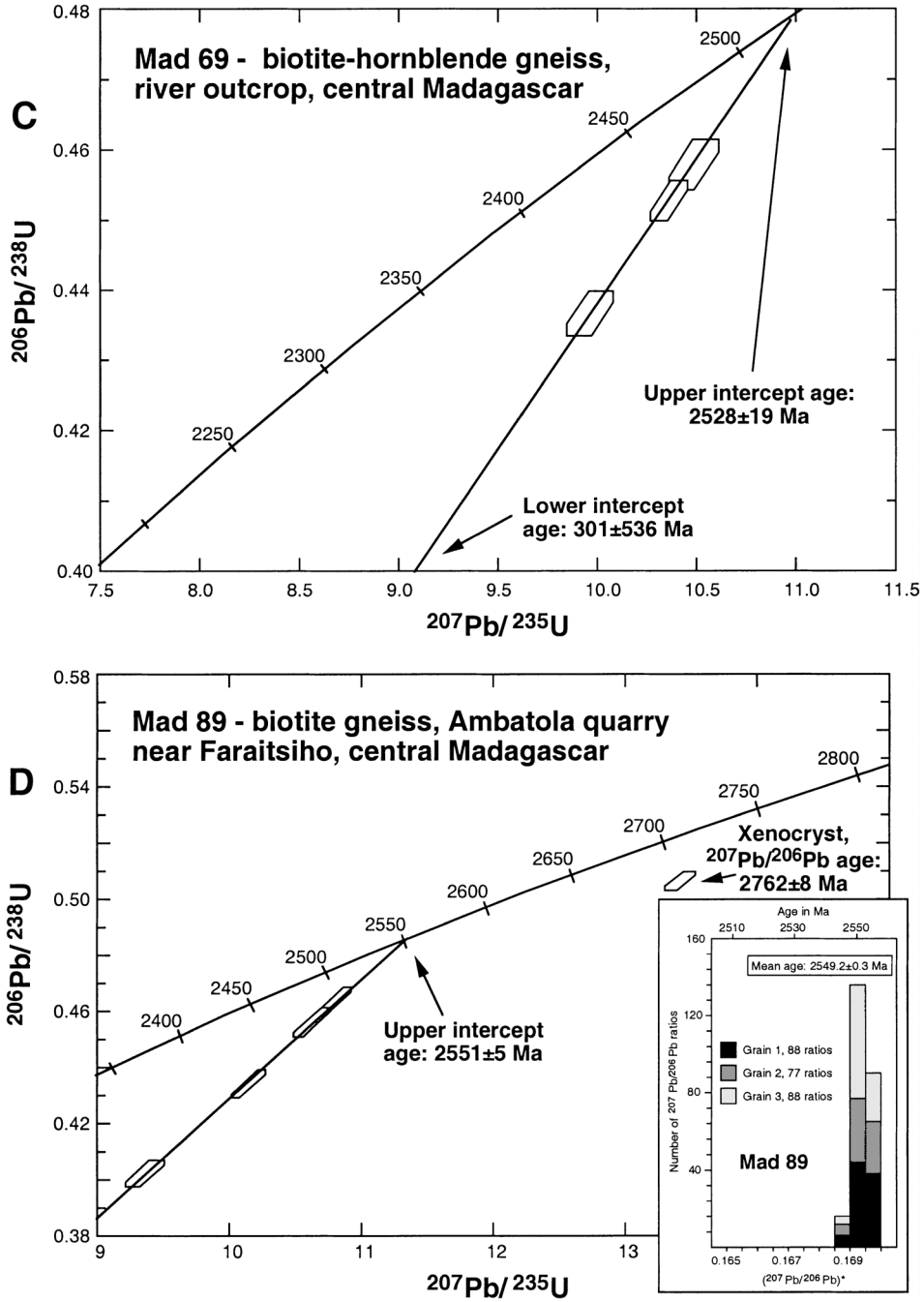

Fig. 8. Concordia diagrams showing analytical data for SHRIMP II analyses of zircons from granitoid gneisses of central Madagascar. Data boxes as in figure 6. (A) Enderbitic gneiss sample Mad 64; (B) enderbitic gneiss sample Mad 65, distribution of late Archean grains. Inset shows histogram with distribution of radiogenic lead isotope ratios derived from evaporation of five zircon grains from same sample, integrated from 539 ratios. (C) biotite-hornblende (quartz monzodioritic) gneiss sample Mad 69; (D) granodioritic gneiss sample Mad 89. Inset shows distribution of radiogenic lead isotope ratios derived from evaporation of three zircon grains from same sample, integrated from 242 ratios.

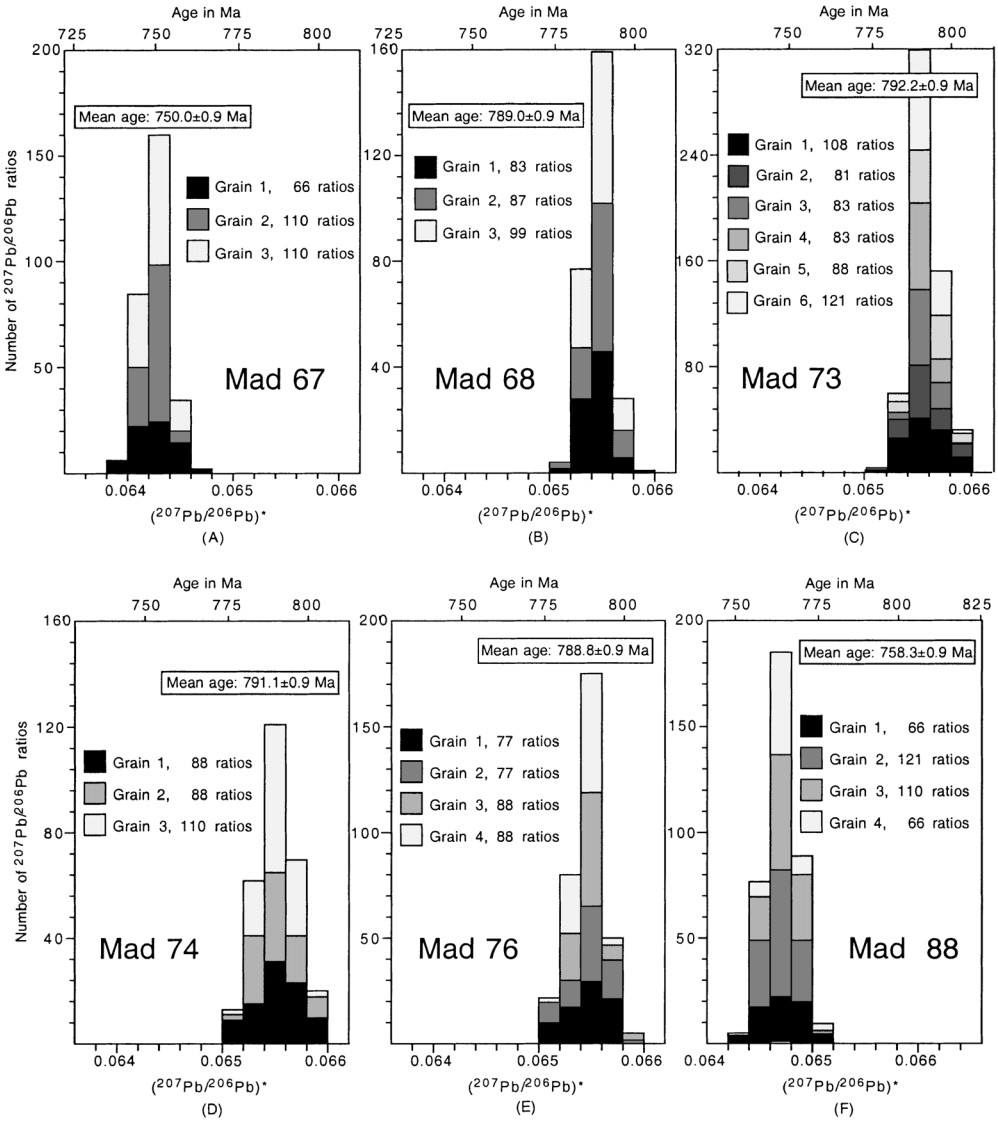

Fig. 9. Histograms showing distribution of radiogenic lead isotope ratios derived from evaporation of single zircons from high-grade gneisses from the area east of Antananarivo, central Madagascar. (A) Spectrum for 3 igneous grains from strongly foliated granitic augen gneiss sample Mad 67, integrated from 286 ratios; (B) spectrum for 3 igneous grains from strongly foliated, coarse-grained, granitic augen gneiss sample Mad 68, integrated from 269 ratios; (C) spectrum for 6 igneous grains from granite gneiss sample Mad 73, integrated from 564 ratios; (D) spectrum for 3 igneous grains from coarse garnetiferous granite gneiss sample Mad 74, integrated from 286 ratios; (E) spectrum for 4 igneous grains from trondhjemitic gneiss sample Mad 76, integrated from 260 ratios; (F) spectrum for 4 grains from strongly foliated adamellitic augen gneiss sample Mad 88, integrated from 363 ratios.

are medium to dark brown, long-prismatic with very well rounded terminations and display well preserved magmatic zonation. Three grains were analyzed on SHRIMP II and produced discordant results (table 4; fig. 8C) which can be fitted to a chord intersecting concordia at 2528±19 and 301±536 Ma (essentially a zero intercept) respectively. We interpret this late Archean age as representing the time of formation of

the original quartz monzodiorite from which sample Mad 69 was derived. The outcrop appearance and zircon morphology are indistinguishable from the orthogneisses so far recognized. Poor outcrop conditions do not make it possible to establish the direct field relationships between gneisses of the ~750 Ma age domain (for example, Mad 68) and the present sample, and we shall discuss this problem in detail in the conclusions section.

Next is Mad 76, a coarse-grained quartz syenite gneiss (table 2) from a roadcut along RN2 west of Ranomafana (table 1; fig. 2). The zircons are clear to light gray, long-prismatic and rounded at their terminations. Four grains were evaporated and yielded identical $^{207}Pb/^{206}Pb$ ratios with a mean age of 788.8±0.9 Ma (table 3; fig. 9E). We interpret this as the time of emplacement of the original quartz syenite. The $\epsilon_{Nd(t)}$ value for whole-rock sample Mad 76 is -14.6, and this results in a mean crustal residence age of 2.54 Ga (table 5). Derivation of the gneiss precursor from Archean crust is most likely as in most previous sample.

The easternmost samples collected on our traverse come from the Brickaville quarry on RN2 (fig. 2), where two types of granitic gneisses are exposed. The older type, represented by Mad 73, is a gray, fine-grained, well foliated granite-gneiss intruded by a coarse, garnetiferous gneissic granite (tables 1 and 2) with flaser texture (Mad 74) and with pods of hornblende and garnet-hornblende aggregates. We suspect that these pods are retrograded garnet-orthopyroxene symplectites.

The zircon populations in these samples are distinctly different from each other in morphology. While Mad 73 contains yellow-brown, long-prismatic grains with well rounded terminations, those of Mad 74 are clear, also long-prismatic but only slightly rounded at their ends. Evaporation of six grains from Mad 73 yielded uniform $^{207}Pb/^{206}Pb$ ratios with a mean age of 792.2±0.9 Ma (table 3; fig. 9C), and three grains from Mad 74 are also isotopically homogeneous and produced a virtually identical age of 791.1±0.9 Ma (table 3; fig. 9D). We interpret these ages as reflecting two phases of a composite granitoid pluton, again underlining the regional importance of the granite-forming event at ~824 to 720 Ma as represented by many of the samples discussed above.

The $\epsilon_{Nd(t)}$ values for whole-rock samples Mad 73 and 74 are -16.2 and -14.4, respectively, while the mean crustal residence ages are 2.66 and 2.53 Ga (table 5). As in most previous cases, this suggests an Archean crustal source for the gneiss protoliths.

GRANITES AND GRANITOID GNEISSES SOUTHWEST AND SOUTH OF TANA

Two samples were collected from an area about 100 km southwest of Tana. Sample Mad 88 is a strongly foliated biotite augen gneiss of adamellitic composition (table 2), collected west of Faratsiho near the village of Mandriarika (table 1, fig. 2). The zircons are uniformly clear to light yellow, long-prismatic with rounded terminations. Evaporation of four grains produced a mean $^{207}Pb/^{206}Pb$ age of 758.3±0.9 Ma (table 3; fig. 9F) considered to reflect the time of emplacement of the gneiss protolith.

Mad 89 is a sample of granodioritic gneiss (table 2) from the Ambatola quarry 7 km northwest of Faratsiho (table 1; fig. 2). The zircons are clear to light gray, long-prismatic with slightly rounded terminations. Five grains were analyzed on SHRIMP II and are all discordant (table 4). Four grains are aligned along a chord (MSWD = 0.63) with concordia intercept ages at 2550±10 and -10±218 Ma, while grain 65-5 is much older and has a $^{207}Pb/^{206}Pb$ age of 2762±8 Ma (fig. 8D). Evaporation of three additional grains yielded a combined mean $^{207}Pb/^{206}Pb$ age of 2549.2±0.3 Ma (table 3; fig. 7D, inset), and we adopt an age of 2550 Ma as most closely reflecting the time of emplacement of the original granodiorite from which gneiss sample Mad 89 was derived. The 2762 Ma grain is interpreted as a xenocryst derived from the gneiss protolith.

Mad 99 is a homogeneous, virtually unfoliated quartz monzonite (table 2) lying directly beneath a major extensional detachment (the Betsileo shear zone; Collins and others, 2000) southwest of Manandona (table 1; fig. 2). The zircons are yellowish to pale brown, long-prismatic with slight rounding at their terminations and weak magmatic zonation. Six grains were analyzed on SHRIMP II (table 4) and display a heterogeneous age distribution. Three grains can be fitted to a chord (MSWD = 5.29) intersecting concordia at 770±18 and 77±233 Ma (fig. 10A). The mean $^{207}Pb/^{206}Pb$ age of these grains is 767±15 Ma. Two additional grains that are optically indistinguishable from the others are much older. Grain 99-4 is concordant at 2502±5 Ma, whereas grain 99-6 is about 10 percent discordant and has a $^{207}Pb/^{206}Pb$ age of 2501±11 Ma (not shown on diagram). The combined mean $^{207}Pb/^{206}Pb$ age of these two grains is 2502±0.5 Ma. Grain 99-1 is also discordant (not shown in diagram) and has a $^{207}Pb/^{206}Pb$ age of 1185±38 Ma. We consider the age of 770 Ma to reflect the time of emplacement of the quartz monzonite pluton prior to formation of the Betsileo shear zone, whereas the three older grains are interpreted as inherited material, either derived from the source region or enclosed in the magma during ascent. The late Archean age of 2502 Ma is similar to that of sample Mad 65 and supports the fact that Archean material probably constitutes much of the lower crust of Madagascar, as also indicated by the Nd isotopic systematics. The Kibaran/Grenvillian age of 1185 Ma for Grain 99-1 is also not surprising, since similar xenocryst ages were found in samples Mad 60, 62, 104, 117 as well as M1 discussed below.

Mad 102 represents an unfoliated and non-retrogressed, coarse-grained enderbite pluton of quartz dioritic composition (table 2), and the sample was collected in the Iarinoro-Tsarasaotra quarry just south of Ilaka (table 1; fig. 2). The zircons are clear, long-prismatic, and euhedral with only slight rounding at their terminations. Four grains were evaporated, of which three produced identical $^{207}Pb/^{206}Pb$ ratios that combine to a mean age of 554.4±1.0, whereas the fourth grain has an older age of 666.2±2.3 Ma (table 3; fig. 11A, B). Since the zircon morphology is typical of an igneous origin, we interpret the age of 554 Ma to reflect the time of pluton emplacement. However, we are not certain whether the enderbite is a primary igneous rock that intruded as dry melt or whether it is the result of *in-situ* transformation as is common in other parts of central Madagascar. In any case, the date of 554 Ma sets a younger age limit to the deformation in this region.

Sample M1 was collected from an undeformed granite of adamellitic composition (table 2) 9 km south of Ivato village on RN 5 (table 1; fig. 2). The zircons are light gray, long-prismatic with well rounded terminations, probably due to metamorphic recrystallization during the high-grade Pan-African event at ~550 to 560 Ma. Four grains were evaporated of which three yielded consistent $^{207}Pb/^{206}Pb$ ratios that combine to a mean age of 589.1±1.0, whereas the fourth grain has an age of 1056.7±1.5 Ma (table 3; fig. 11C, D). As in the previous cases, we consider the younger age represented by three grains to reflect the time of adamellite emplacement. Grain 4 is interpreted as a xenocryst and provides further evidence for the existence of Kibaran/Grenvillian crustal material at depth.

Sample Mad 103 is a dark hornblende-biotite gneiss of quartz monzodioritic composition (table 2) that was collected 6 km south of Ambositra (table 1; fig. 2). Gneissic foliation dips regularly at 56° to the west and is locally cut by 1 to 3 cm wide granite veins. The zircons are clear to light gray, long-prismatic with slightly rounded terminations. Six grains were analyzed on SHRIMP II, of which five analyses are tightly grouped and near-concordant at 2514±6 Ma while one grain is significantly discordant (table 4; fig. 10B). Evaporation of six other grains yielded a mean $^{207}Pb/^{206}Pb$ age of 2514.4±0.2 Ma (table 3; fig. 10B, inset), identical to the ion-microprobe result. We consider the age of 2514 Ma to reflect the emplacement age of the monzodioritic gneiss precursor.

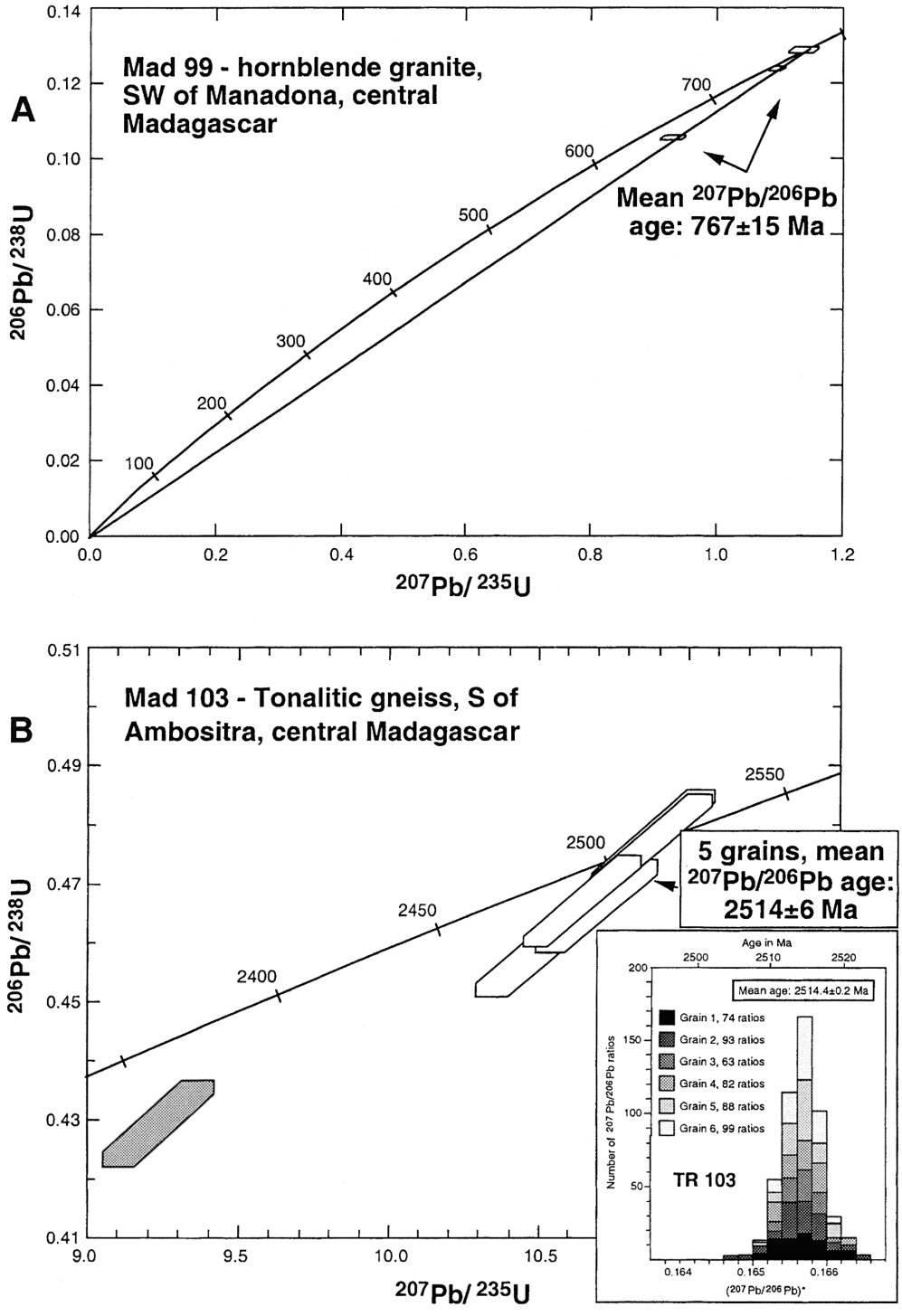

Fig. 10. Concordia diagram showing analytical data for SHRIMP II analyses of zircons from granites and gneisses from central Madagascar. Data boxes as in figure 5. (A) Quartz monzodioritic gneiss sample Mad 99; (B) quartz monzodioritic gneiss sample Mad 103. Inset shows distribution of radiogenic lead isotope ratios derived from evaporation of 6 zircon grains from same sample, integrated from 499 ratios.

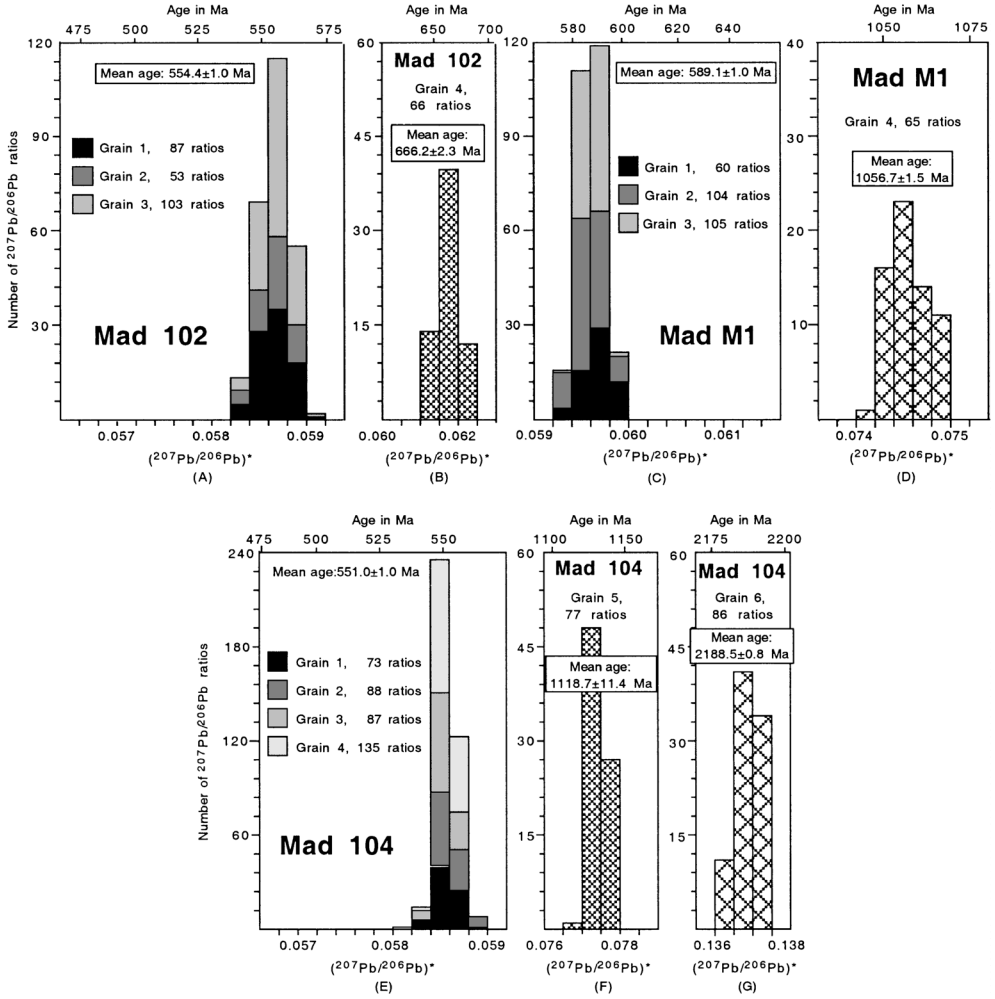

Fig. 11. Histograms showing distribution of radiogenic lead isotope ratios derived from evaporation of single zircons from high-grade gneisses from central Madagascar. (A) Spectrum for 3 grains from charnockite sample Mad 102, integrated from 243 ratios; (B) spectrum for xenocrystic grain from same sample; (C) spectrum for 4 igneous grains from retrogressed charnockitic gneiss sample Mad 104, integrated from 383 ratios; (D, E) spectra for xenocrystic grains from same sample; (F) spectrum for 3 grains from undeformed granite sample Mad M-1, integrated from 269 ratios; (G) spectrum for xenocrystic grain from same sample.

Lastly, sample Mad 104 was collected about 2 km north of Ivato village, at a road junction 15 km south of Ambositra (table 1; fig. 2) and is a leucocratic, foliated biotite gneiss of granitic composition (table 2). The zircons are light gray, long-prismatic with well rounded terminations. Four grains produced consistent $^{207}Pb/^{206}Pb$ ratios with a mean age of 551.0± 1.0 Ma, while two additional grains of similar morphological appearance yielded ages of 1118.7±1.4 and 2188.5±0.8 Ma (table 3; fig 11E-G). We consider the age of 551 Ma to reflect the original granite emplacement, whereas the two older grains are probably xenocrysts inherited from the source region of the granite. This granitic gneiss was derived from a crustal melt apparently emplaced during the peak of high-grade metamorphism in the region and, because the rock is well foliated, the age demonstrates that deformation continued after emplacement.

SIGNIFICANCE OF WHOLE-ROCK GEOCHEMISTRY AND HND ISOTOPIC SYSTEMATICS

The granitoids of the Antananarivo Block dated in this study reflect a spectrum of compositions ranging from peraluminous granodiorites to granites, with minor quartz diorites. All have trace element characteristics resembling those in magmatic arcs, that is, negative Nb, Ti, and Zr anomalies (table 3), which is in marked contrast to the younger stratoid granites (Nédélec and others, 1994). However, arc-like element patterns are also a characteristic feature of high-grade granitic crust in general (Wilson, 1989) and are not diagnostic for a particular tectonic setting. For example, plume generated melting of continental crust would also produce compositions similar to those generated in arc environments. However, in a plume environment one would expect voluminous basic magmatism showing the characteristic chemical fingerprint of a mantle plume (see Fitton and others, 1997). In the Antananarivo block there is a marked scarcity of basic plutons in the 850 to 700 Ma age range, and none of the granitoid rocks preserve any chemical signature of a plume, arguing against the direct involvement of a mantle plume in their generation.

The T_{DM} Nd mean crustal residence ages and $\epsilon_{Nd(t)}$-values summarized in table 4 are graphically presented in the Nd evolution diagram of fig. 12 and reflect participation of significant volumes of early Proterozoic to late Archean crust in the generation of the granitoids. The presence of juvenile additions to the crust in several samples is not excluded by these data but must be minor. The Nd isotopic data are consistent with the zircon xenocryst age pattern and with similar Nd isotopic systematics reported by Handke, Tucker, and Ashwal (1999) for granitoid rocks in the Itremo region in west-central Madagascar. Our Nd isotopic systematics and zircon ages effectively rule

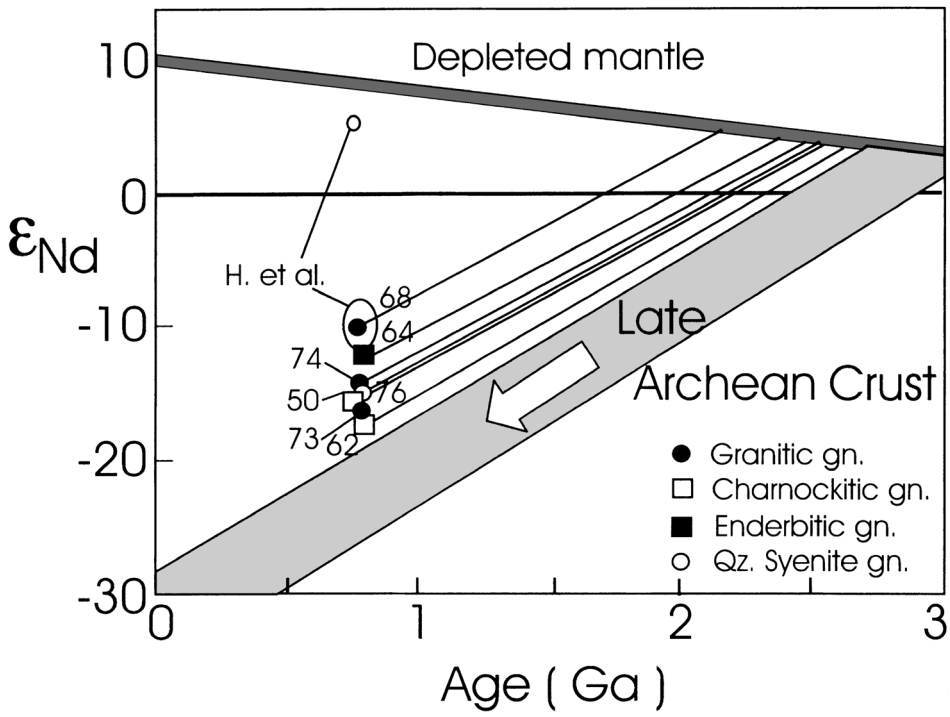

Fig. 12. Nd evolution diagram showing positions of samples analyzed in this study. For analytical data, see table 3. Depleted mantle line after DePaolo (1981).

out intraoceanic magmatic arc scenarios for the granitoid rocks of central Madagascar. The available evidence suggests that these granitoids were produced by intracrustal melting resulting either from magmatic underplating or fluid infiltration at an Andean-type active continental margin. These scenarios are further explored below.

DISCUSSION AND CONCLUSIONS

The zircon ages of this study suggest three distinct periods of granitoid magmatism and/or high-grade metamorphism in central Madagascar at ~570 to 530, ~824 to 720, and 2520 to 2500 Ma, respectively and the presence of unspecified amounts of Paleo- to Mesoprozerozoic crustal material as revealed by the presence of zircon xenocrysts (fig. 13). A similar age pattern has also been recorded over an even larger area by Tucker and others (1997). Our zircon ages and Nd isotopic systematics permit the following conclusions to be drawn concerning the Neoproterozoic history of central Madagascar.

1. There was a massive and widespread magmatic event that produced granitoid rocks during the period ~824 to ~720 Ma (at maximum uncertainty; fig. 13). These granitoids, on the basis of their Nd isotopic systematics, were the product of melting of older continental crust ranging in age from late Archean to Mesoproterozoic (fig. 12). A minor component of juvenile material is not excluded by the Nd isotopic systematics. This could have been supplied either during an extensive plume-related underplating event, by mantle-delamination or by magmatism within a continental arc.

A plume impinging on the base of the crust would provide the heat source to enable extensive melting of the continental crust above. However, characteristic geochemical signatures of mantle plumes (see Fitton and others, 1997) are missing from the Madagascan 824 to 720 Ma granitoid intrusions. In areas above mantle plumes, voluminous basic intrusions generally occur from adiabatic melting of the depressurized mantle beneath. Basic intrusions are, however, rare in central Madagascar, thus a plume model is hard to reconcile with the available observations.

Delamination of a mantle keel is another possible mechanism for emplacing hot material onto the base of the crust. Most models invoking this process require delamination following crustal thickening. However, in Madagascar there is no evidence for a

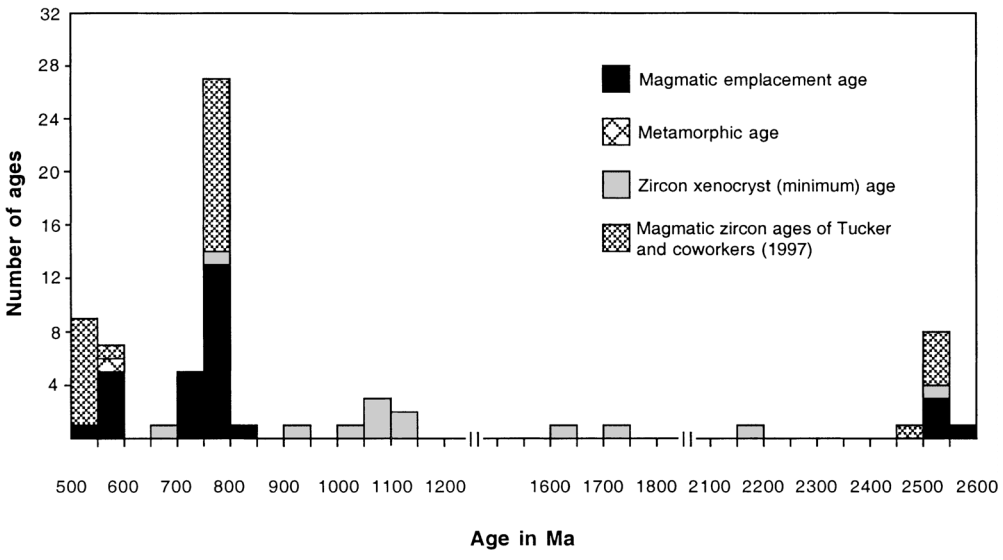

Fig. 13. Histogram showing distribution of zircon ages in central Madagascar.

major orogenic episode prior to the intrusion of the granitoids, which would have provided the trigger for mantle delamination.

Neoproterozoic subduction would provide a plausible mechanism for producing large volumes of granites. In such a model, the inheritance recorded from the Nd-isotopes would suggest subduction beneath an Archean to early Proterozoic block. Although the trace element signatures are not unique, the range of lithologies (diorites to granites) and the chemistry of the intrusions would be consistent with such a setting. Our age data are also not sufficient to state whether there was continuous granitoid emplacement for ~104 Ma between ~824 and 720 Ma, or whether there were distinct pulses within this range.

Handke, Tucker, and Ashwal (1999) analyzed gabbroic intrusives that were coeval with granitoid plutons (779-804 Ma) in the Itremo thrust sheet (figs. 1, 2). From the geochemical compositions they concluded that these rocks were intruded in an Andean-type arc setting, approximately synchronous with the breakup of Rodinia, and resulted from subduction of Mozambique oceanic lithosphere under the west-central part of the island. However, as argued below, the field relations of the rocks we sampled as well as the age data do not support a position of Madagascar next to India and marginal to Rodinia between 824 and 720 Ma ago as suggested by Handke, Tucker, and Ashwal (1999). Also, our Nd isotope systematics show little, if any, evidence for a subduction-related component.

An intrusion event similar in time to that in central Madagascar was also identified in northern Somalia, an area close to Madagascar in a Gondwana position (fig. 14), and where gabbroid and granitoid magmas were emplaced into older continental crust between ~840 and ~720 Ma ago (Kröner and Sassi, 1996). Farther south, in Kenya and Tanzania, there are no reliable published emplacement ages for the precursor rocks of the vast gneissic terrain making up the central part of the East African orogenic belt, but new zircon ages from the region north-west of Dar es Salaam suggest granitoid rocks, about 800 to 840 Ma in age, to be tectonically interlayered with 2700 to 2600 Ma old tonalitic-trondhjemitic gneisses (Muhongo, Kröner, and Nemchin, in press; fig. 14). In southern Malawi, granitoid gneisses and charnockites are widespread and have protolith zircon ages ranging from ~1040 to ~580 Ma (fig. 14) with no apparent cluster of ages as in the Madagascar range (Kröner and others, in press). In northern Mozambique, voluminous granitoid rocks were emplaced between ~850 and 1100 Ma (based on Rb-Sr and zircon dating, see summaries in Pinna and others, 1993; Kröner and others, 1997). These are older and outside the age range established for the Madagascar Block. In northern Zimbabwe, Kibaran as well as early and late Pan-African ages were reported from the Zambezi belt (Barton and others, 1991; Oliver and others, 1998; Dirks and others, 1999; Kröner, Dirks, and Hiemstra, unpublished data). Dirks and others (1999) reported $^{207}Pb/^{206}Pb$ single zircon ages of 794 to 737 Ma for granitoid gneisses of the Makuti Group near Lake Kariba, whereas Barton and others (1991) obtained Rb-Sr whole-rock isochron ages ranging from 955 to 605 Ma, with a concentration between 877 and 786 Ma. They interpreted the latter range as reflecting the peak of an early Pan-African plutonic-metamorphic event.

There are no known rocks of the age range 824 to 720 Ma in southwestern India (fig. 14, see also compilation in Bartlett and others, 1998), and there is little resemblance in the rock types between central Madagascar and the Madurai and Nilgiri Blocks of southern India. The crystalline basement in this part of India is composed of late Archean gneisses subjected to high-grade metamorphism around 2500 Ma ago and with a high-grade metamorphic event in the far south during late Neoproterozoic times (see summaries in Jayananda and others, 1995; Jayananda and Peucat, 1996; Bartlett and others, 1998; and Raith and others, 1999). This lack of ~824 to 720 Ma magmatism is surprising as most reconstructions of Gondwana juxtapose southwestern India with

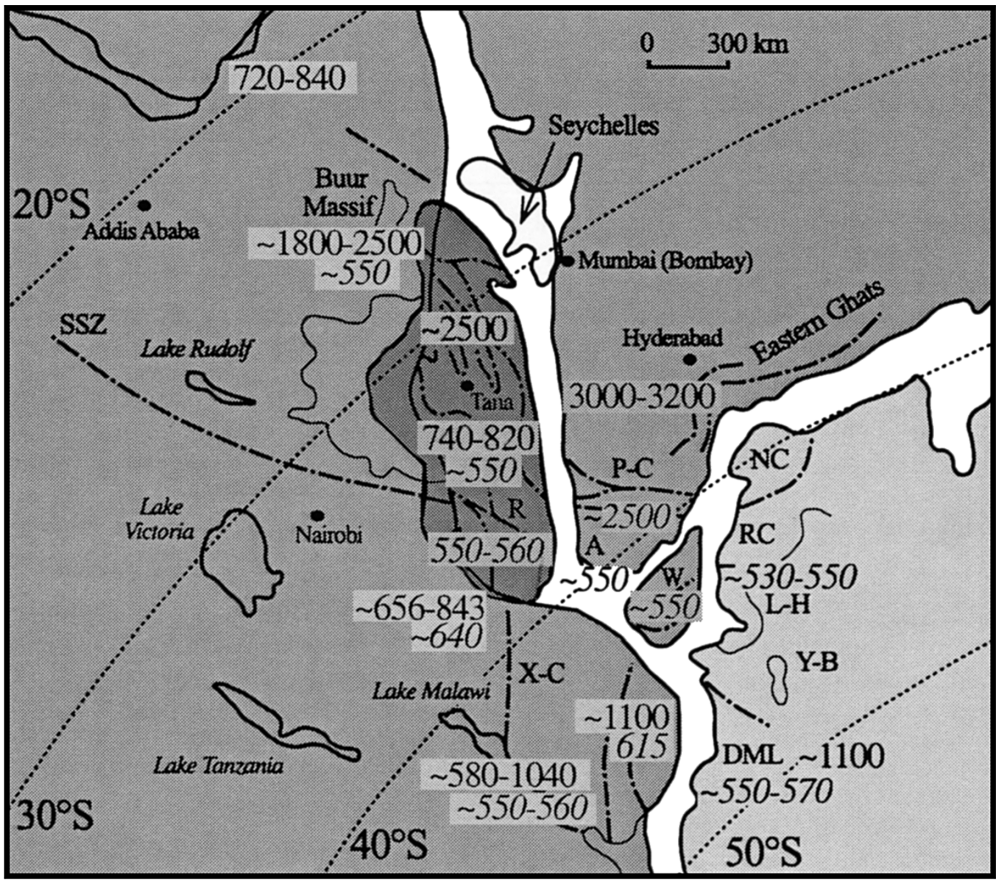

Fig. 14. Popular "tight fit" Gondwana reconstruction after Lawver and others (1992) showing position of Madagascar with respect to East Africa and India at 200 Ma. Note that major shear zones in Madagascar appear to join up with similar structures in southernmost India and East Africa, but age provinces do not correlate well. Paleolatitudes reconstructed for 200 Ma after Lawver and others (1992). Y-B = Yamato-Belgica Complex; L-H = Lützow-Holm Complex; RC = Rayner Complex; NC = Napier Complex; P-C = Palghat-Cauvery shear zone; A = Achankovil shear zone; R = Ranotsara shear zone; SSZ = Surma shear zone; DML = Dronning Maud Land; X-C = Xixano-Chiwaro shear zone. Regular numbers indicate zircon ages (in Ma) for magmatic events, italic numbers are for zircon ages signifying metamorphic events.

Madagascar and link the Ranotsara shear zone of Madagascar with either the Achankovil shear zone (Windley and others, 1994; Windley and Razakamanana, 1996) or the Palghat-Cauvery shear zone farther north (De Wit, Vitali, and Ashwal, 1995; Harris and others, 1996). Thus, simple reconstructions based on major shear zones alone may not be correct. In contrast, the amphibolite- to granulite-facies Wanni Complex of Sri Lanka preserves I-type granitoid intrusions dated as 750 to 790 Ma (Kröner and Jaeckel, 1994) and is thrust over the ~650 to 2000 Ma Highland Complex to the east (Kröner and others, 1996). The timing of intrusion and chemical composition of these granitoids is similar to those found in central Madagascar, as is the structural setting since both regions have a coeval terrane thrust over a significantly older terrane.

2. The recognition of high-grade metamorphism and granitoid magmatism in central Madagascar at ~550 Ma (fig. 13) confirms earlier suggestions that this event affected large parts of the island 560 to 550 Ma ago and caused extensive granulite-facies

metamorphism. This event is structurally related to widespread extensional deformation (Windley and Razakamanana, 1996; Collins and others, 2000) that post-dates the "docking" of the island with eastern Africa during a collisional event that generated the Mozambique belt (Stern, 1994; Windley and others, 1994; Kröner, Braun, and Jaeckel, 1996; Kröner and others, 1999; Collins, Razakamanana, and Windley, 2000). Coeval or slightly older granulite-facies metamorphism is found in southern Madagascar (Paquette and others, 1994; Kröner, Braun, and Jaeckel, 1996; Ito, Suzuki, and Yogo, 1997). Paquette and Nédelec (1998) suggest that collisional deformation and metamorphism occurred between 700 to 650 Ma. Our dating of the granulite event does not disprove this, as the metamorphism is coeval with extensional deformation. However, it does highlight the need for more detailed structural/metamorphic/geochronological studies to elucidate the tectonic evolution of this key part of Gondwana.

Elsewhere in the East African orogenic belt, granulite-facies metamorphic zircons were dated as 615±3 Ma in northern Mozambique (Kröner and others, 1997b) and at 640 Ma in central Tanzania (Muhongo, Kröner and Nemchin, in press; see fig. 14). Approx 650 Ma (Rb-Sr) metamorphic ages were obtained from Eritrea by Beyth and others (1997). These ages have all been interpreted as representing the timing of collision between East and West Gondwana and are all significantly older than the metamorphic zircon ages found in Madagascar. In southern India, studies of charnockites close to the Achankovil shear zone have obtained a Sm-Nd mineral isochron age of 539±10 Ma (Santosh and others, 1992), while monazite U-Pb ages of ~540 to 550 Ma have also been obtained from the Trivandrum block of southern India (Buhl, 1987; Braun and others, 1998). In Sri Lanka, peak granulite-facies metamorphism has been dated as between 539±6 and 608±3 Ma. (Kröner and Williams, 1993; Kröner and others, 1996). In East Antarctica, a variety of felsic orthogneisses in Dronning Maud Land has yielded Grenvillian-type SHRIMP U-Pb zircon ages between 1073 and 1137 Ma, but the area has also been affected by Pan-African magmatism between 608 and 530 Ma ago, and the zircons reflect two periods of high-grade metamorphism at 570 to 550 and 530 to 515 Ma respectively (Jacobs and others, 1998). Farther north, in the Yamato-Belgica Complex and the Lützow-Holm Complex, there is evidence for granitoid magmatism and granulite facies metamorphism at 520 to 550 Ma (Shiraishi and others, 1994).

The southern Indian, Sri Lankan, and East Antarctic ages for peak metamorphism are in close agreement with the Madagascar results, suggesting that these terranes were proximal to each other during high-grade metamorphism (fig. 14). This also supports previous suggestions linking these three terranes in a common Pan-African history of terrane amalgamation (Kröner, 1991; Kriegsman, 1993; Windley and others, 1994; Windley and Razakamanana, 1996).

3. Since all the granitoid gneisses investigated in this study seem to belong to the same structural domain with predominant west-dipping foliations, deformation of the high-grade rocks of the Antananarivo Block is constrained between ~551 Ma, the youngest granitoid gneiss dated in this study, and ~538 Ma, the age for the post-tectonic and undeformed Carion granite. The Archean gneisses were completely reconstituted structurally and, in our view, form thrust sheets within the Pan-African granitoid assemblage.

4. The lack of direct evidence for magmatic activity or evidence for deformation in Madagascar within the Kibaran-Grenvillian age range (1000-1300 Ma, see fig. 13) is notable as it implies that Madagascar lay in a relatively quiescent tectonic position during the amalgamation of the pre-Gondwana supercontinent Rodinia and was not involved in collisional tectonics at that time (note, however, the rare zircon xenocrysts dated between 1006 and 1057 Ma). This is surprising in view of the fact that most current reconstructions of Rodinia place the island in a marginal position attached to the west coast of India and consider it as a Kibaran/Grenvillian crustal element (Hoffman, 1991;

Dalziel, 1991, 1997; Unrug, 1996; Torsvik and others, 1996). If these reconstructions are correct, then this margin of Rodinia must have been a passive or transform margin. Other alternatives exist, however, including that Madagascar inhabited a more central position within Rodinia, or that it was attached to the east coast of Africa (Cox and others, 1998), or that it formed a separate microcontinent within the Mozambique Ocean. With age data alone we are unable to make any more definite suggestions; however, field and structural relationships imply that one of the final two alternatives is the most likely (see below).

5. The late Archean ages in central Madagascar (between 2550 and 2500 Ma, fig. 13), show that at least some of the Neoproterozoic granitoids were derived from an Archean source, and the late Archean zircon ages reported by Tucker and others (1999) from the northern and western part of the island reveal the presence of a substantial segment of old crust whose origin remains uncertain. There are no known Archean ages in Somalia (the 2500 Ma age shown in fig. 14 for the Buur Massif is based on a single upper intercept of 2514±44 Ma for highly discordant data, Lenoir and others, 1994), and the eastern Mozambique belt in Kenya is largely composed of Mesoproterozoic rocks (Key and others, 1989; Mosley, 1993). However, new data from the high-grade terrain of central Tanzania suggest the presence of late Archean granitoid gneisses that may be reworked equivalents of the Dodoma or Tanzania craton to the West (Muhongo, Kröner and Nemchin, in press). A link between the Madagascan Archean crust and East African crust is one possibility, but a link with the Nilgiri and Madurai Blocks of southern India (Bernard-Griffiths and others, 1987) is also possible. The problem with the latter suggestion is that there is little resemblance in rock types, structures, and ages between these areas (see summary in Jayandanda and Peucat, 1996); specifically, the late Archean granulite-facies event recorded in the gneisses of southern India (Raith and others, 1999) has so far not been found in central and northern Madagascar.

6. Cox, Armstrong, and Ashwal (1998) interpreted detrital zircon age populations from the Itremo Group of central Madagascar (Itremo thrust sheet in fig. 1) to indicate a link between central Madagascar and East Africa by early Neoproterozoic time. These authors suggested that a suture between the Tanzanian and Dharwar cratons must lie east of the Itremo Group (Cox, Armstrong, and Ashwal, 1998). Although a shear zone (extensional detachment) exists between the Itremo Group and the underlying Antananarivo Block Collins; and others, 2000), there is no evidence of an oceanic suture within it. Throughout the Antananarivo Block, gneissic foliation generally dips toward the west. A thick, highly sheared paragneiss belt containing many entrained mafic and ultramafic blocks and emerald deposits lies in the east separating the Antananarivo block from the Archean Antongil block (fig. 1). Our data suggest that voluminous remelting of Archean and Proterozoic crust over an 104 Ma time period occurred prior to contractional deformation and granulite-facies metamorphism throughout the Antananarivo block. Trace element evidence suggests that this magmatism was related to subduction (Handke and others, 1997, 1999). Combining the structural evidence with the geochemical and geochronological data, we suggest that this metasedimentary belt contains a major suture that represents a west-dipping convergent margin (labeled the Betsimisiraka suture in fig. 1 after the region where it crops out). This margin consumed (at least part of) the Mozambique ocean during the early Neoproterozoic. Central Madagascar lay above this subduction zone between 824 and 720 Ma, during which an Andean-type arc developed. Continued convergence between East and West Gondwana led to the collision of central Madagascar with southern India and possibly also eastern Africa. Based on the remarkable similarities between the chemistry and timing of Neoproterozoic magmatism in Sri Lanka with central Madagascar we suggest that the two islands lay in analogous tectonic positions at the time. Granulite-facies metamorphism occurred throughout Madagascar, southern India, and Sri Lanka after suturing of East and West Gondwana at ~550 Ma.

ACKNOWLEDGMENTS

This study was funded by the Deutsche Forschungsgemeinschaft (grant Kr 590/36 to A.K.) and by NERC grant GR9/1041 to B.F.W. A.S.C. thanks the trustees of the Fermor Fellowship for funding his participation in this work, the University of Leicester, and the Tectonics Special Research Centre (TSRC) in Perth for providing research facilities. A.S.C.'s authorship forms TSRC contribution #75. Some of the zircon analyses were carried out on the Sensitive High Resolution Ion Microprobe mass spectrometer (SHRIMP II) operated by a consortium consisting of Curtin University of Technology, the Geological Survey of Western Australia, and the University of Western Australia with the support of the Australian Research Council. We appreciate the advice of A. Kennedy and D. Nelson during SHRIMP analysis and data reduction. The comments and suggestions for improvement of the manuscript by R.J. Stern, M.J. Handke, and an anonymous referee are appreciated.

REFERENCES

Arndt, N.T., and Goldstein, S.L., 1987, Use and abuse of crust-formation ages: Geology, v. 15, p. 893-895.

Ashwal, L.D., and Tucker, R.D., 1997, Archean to Neoproterozoic events in Madagascar: Implications for the assembly of Gondwana: Terra Nova, v. 9, Abstract Supplement 1, p. 163-164.

Bartlett, J.M., Dougherty-Page, J.S., Harris, N.B.W., Hawkesworth, C.J., and Santosh, M., 1998, The application of single zircon evaporation and model Nd ages to the interpretation of polymetamorphic terrains: an example from the Proterozoic mobile belt of south India: Contributions to Mineralogy and Petrology, v. 131, p. 181-195.

Barton, C.M., Carney, J.N., Crow, M.J., Dunkley, P.N., and Simango, S., 1991, The geology of the country around Rushinga and Nyampanda: Zimbabwe Geological Survey, Bulletin 92, 220 p.

Baur, N., Kröner, A., Liew, T. C., Todt, W., Williams, I. S. and Hofmann, A. W., 1991, U-Pb isotopic systematics of zircons from prograde and retrograde transition zones in high-grade orthogneisses, Sri Lanka: Journal of Geology, v. 99, p. 527-545.

Bernard-Griffiths, J., Jahn, B.M., and Sen, S.K., 1987, Sm-Nd isotopes and REE geochemistry of Madras granulites: an introductory statement: Precambrian Research, v. 37, p. 343-355.

Besairie H., 1968-1971, Description géologique du massif ancien de Madagascar. Document Bureau Géologique Madagascar. no. 177. and no. 177a: centre nord et centre nord-est; 177b: région côtière orientale; 177c: région centrale- système du graphite; 177d: région centrale–système du Vohibory; 177e: le sud; 177f: le nord: Bureau Géologique Madagascar.

——— 1973, Carte géologique à 1\2000000 de Madagascar. Service Géologique de Madagaskara. Antananarivo.

Beyth, M., Stern, R.J., and Matthews, A., 1997, Significance of high-grade metasediments from the Neoproterozoic basement of Eritrea: Precambrian Research, v. 86, p. 45-58.

Braun, I., Montwel, J.-M., and Nicollet, C., 1998, Electron microprobe dating of monazites from high-grade gneisses and pegmatites of the Kerala khondalite belt, southern India: Chemical Geology, v. 146, p. 65-85.

Brewer, T.S., Daly, J.S., and Åhäll, K.-I., 1998, Contrasting magmatic arcs in the Palaeoproterozoic of the south-western Baltic Shield: Precambrian Research, v. 92, p. 297-315.

Buhl, D. ms, 1987, Ub-Pb und Rb-Sr Altersbestimmungen und Untersuchungen zum StrontiumIsotopenaustausch an Granuliten Südindiens: Doctoral dissertation, University of Münster, Germany.

Claoué-Long, J.C., Compston, W., Roberts, J., and Fanning, C.M., 1995, Two Carboniferous ages: a comparison of SHRIMP zircon dating with conventional zircon ages and $^{40}Ar/^{39}Ar$ analyses: Society of Sedimentary Geology, Special Publication 54, p. 3-21.

Cocherie, A., Guerrot, C., and Rossi, P., 1992, Single-zircon dating by step-wise Pb evaporation; comparison with other geochronological techniques applied to the Hercynian granites of Corsica, France: Chemical Geology, Isotope Geoscience Section, v. 101, p. 131-141.

Collins, A.S., Razakamanana, T., and Windley, B.F., 2000, Neoproterozoic crustal-scale extensional detachment in central Madagascar: implications for extensional collapse of the East African Orogen: Geological Magazine, v. 137, p. 39-51.

Compston, W. Williams, I.S. Kirschvink, J.L.Zhang, Z., and Ma, G., 1992, Zircon U-Pb ages for the Early Cambrian time scale: Journal of the Geological Society of London, v. 149, p. 171-184.

Condie, K.C., Boryta, M.D., Liu Jinzhuong, and Qian Xianglin, 1993, The origin of khondalites: Geochemical evidence from the Archean to early Proterozoic granulite belt in the North China craton: Precambrian Research, v. 59, p. 207-223.

Cox, R., and Armstrong, R.A., 1997, Geochronology and provenance of the Itremo Group, central Madagascar, in UNESCO-IUGS-IGCP-348/368 International Field Workshop on Proterozoic geology of Madagascar: Johannesburg, South Africa, Gondwana Research Group, Proceedings, Miscellaneous Publication 5, 99 p.

Cox, R., Armstrong, R.A., and Ashwal, L.D., 1998, Sedimentology, geochronology and provenance of the Proterozoic Itremo Group, central Madagascar, and implications for pre-Gondwana palaeogeography: Journal of the Geological Society of London, v. 155, p. 1009-1024.

Dalziel, I.W.D., 1991, Pacific margins of Laurentia and East Antarctica-Australia as a conjugate rift pair: Evidence and implications for an Eocambrian supercontinent: Geology, v. 19, p. 598-601.
——— 1997, Neoproterozoic-Palaeozoic geography and tectonics: review, hypothesis, environmental speculation: Geological Society of America Bulletin, v. 109, p. 16-42.
Debon, F., and Le Fort, P., 1982, A chemical-mineralogical classification of common plutonic rocks and associations. Transactions of the Royal Society of Edinburgh, v. 73, p. 135-150.
De Laeter, J.R., and Kennedy, A.K., 1998, A double focusing mass spectrometer for geochronology: International Journal of Mass Spectrometry and Ion Processes, v. 178, p. 43-50.
DePaolo, D.J., 1981, A Nd and Sr isotopic study of Mesozoic calc-alkaline granitic batholiths of the Sierra Nevada and Peninsular Ranges, California: Journal of Geophysical Research, v. 86, p. 10370-10488.
De Wit, Vitali, E., and Ashwal, L., 1995, Gondwana reconstruction of East Africa-Madagascar-India-Sri Lanka-East Antarctica fragments revisited: Geological Society of South Africa, Centennial Congress, Johannesburg, Abstract-volume, p. 218-221.
Dirks, P.H.G.M., Kröner, A., Jelsma, H.A., Sithole, T.A., and Vinyu, M.L., 1999, Structural relations and Pb-Pb zircon ages for the Makuti gneisses: evidence for a crustal-scale Pan African shear zone in the Zambezi Belt, NW Zimbabwe: Journal of African Earth Sciences, v. 28, p. 427-442.
Fitton, J.G., Saunders, A.D., Norry, M.J., Hardarson, B.S., and Taylor, R.N., 1997, Thermal and chemical structure of the Iceland Plume: Earth and Planetary Science Letters: v. 153, p. 197-208.
Handke, M.J., Tucker, R.D., and Ashwal, L.D., 1999, Neoproterozoic continental arc magmatism in west-central Madagascar: Geology, v. 27, p. 351-354.
Handke, M.J., Tucker, R.D., and Hamilton, M.A., 1997, Early Neoproterozoic (800-790 Ma) intrusive igneous rocks in central Madagascar: geochemistry and petrogenesis: Geological Society of America, Abstracts with Programs, v. 29, p. 468.
Harris, N.B.W., Barlett, J.M., and Santosh, M., 1996, Neodymium isotope constraints on the tectonic evolution of East Gondwana: Journal of Southeast Asian Earth Sciences, v. 14, p. 119-125.
Harvey, P.K., 1989, Automated X-ray fluorescence in geochemical exploration, in Ahmedali, editor, X-ray fluorescence analysis in the geological sciences, advances in methodology: Geological Association of Canada, Shourt Course 7, p. 221-257.
Hegner, E., Watter, H.J., and Satir, M., 1995, Pb-Sr-Nd isotopic compositions and trace element geochemistry of megacrysts and melililites from the Tertiary Urach volcanic field: source composition of small-volume melts under SW Germany: Contributions to Mineralogy and Petrology, v. 122, p. 322-335.
Hoffman, P.F., 1991, Did the breakout of Laurentia turn Gondwana inside out? Science, v. 252, p. 1409-1412.
Hottin, G., 1976, Présentation et essai d'interprétation du Précambrien de Madagascar: Bulletin du Bureau de Recherches Géologiques et Minères, 2'eme série, section IV, p. 117-153.
Ito, M, Suzuki, K., and Yogo, S., 1997, Cambrian granulite to upper amphibolite facies metamorphism of post-797 Ma sediments in Madagascar: Nagoya University, Journal of Earth and Planetary Sciences, v. 44, p. 89-102.
Jacobs, J., Fanning, C.M., Henjes-Kunst, F., Oelsch, M., and Paech, H.-J., 1998, Continuation of the Mozambique belt into East Antarctica: Grenville-age metamorphism and polyphase Pan-African high-grade events in central Dronning Maud Land: Journal of Geology, v. 106, p. 385-406.
Jaeckel, P., Kröner, A., Kamo, S. L., Brandl, G., and Wendt, J. I., 1997, Late Archean to early Proterozoic granitoid magmatism and high-grade metamorphism in the central Limpopo Belt, South Africa: Journal of the Geological Society of London, v. 154, p. 25-44.
Jahn, B.-M., and Zhang, Z.-Q., 1984, Radiometric ages (Rb-Sr, Sm-Nd, U-Pb) and REE geochemistry of Archean granulite gneisses from Eastern Hebei Province, China, *in* Kröner, A., Hanson, G.N., and Goodwin,. A.M. editors, Archaean Geochemistry: Berlin, Springer-Verlag, p. 204-234.
Jayananda, M., Janardhan, A.S., Sivasubramanian, P., and Peucat, J.J., 1995, Geochronologic and isotopic constraints on granulite formation in the Kodaikanal area, southern India: Geological Society of India Memoir, v. 34, p. 373-390.
Jayananda, M., and Peucat, J.J., 1996, Geochronological framework of southern India, *in* Santosh, M., and Yoshida, M., editors, The Archean and Proterozoic terrains of southern India within East Gondwana: Japan, Osaka University, Gondwana Research Group Memoir, v. 3, p. 53-75.
Karabinos, P., 1997, An evaluation of the single-grain zircon evaporation method in highly discordant samples. Geochimica et Cosmochimica Acta, v. 61, p. 2467-2474.
Kennedy, W. Q., 1964, The structural differentiation of Africa in the Pan-African (±500 m.y.) tectonic episode: Leeds University, Research Institute on African Geology, Annual Report, v. 8, p. 48-49.
Key, R.M., Charsley, T.J., Hackman, B.D., Wilkinso, A.F., and Rundle, C.C., 1989, Superimposed Upper Proterozoic collision-controlled orogenies in the Mozambique orogenic belt of Kenya: Precambrian Research, v. 44, p. 197-225.
Kinny, P.D., 1986, 3820 Ma zircons from a tonalitic Amitsoq gneiss in the Godthåb district of southern West Greenland: Earth and Planetary Science Letters, v. 79, p. 337-347.
Kober, B.,1986, Whole-grain evaporation for $^{207}Pb/^{206}Pb$-age-investigations on single zircons using a double-filament thermal ion source: Contributions to Mineralogy and Petrology, v. 93, p. 482-490.
——— 1987, Single-zircon evaporation combined with Pb^{+} emitter-bedding for $^{207}Pb/^{206}Pb$-age investigations using thermal ion mass spectrometry, and implications to zirconology: Contributions to Mineralogy and Petrology, v. 96, p. 63-71.
Kretz R., 1983, Symbols for rock-forming minerals: American Mineralogist, v. 68, p. 277-279.
Kriegsman, L.M., 1993, Geodynamic evolution of the Pan-African lower crust in Sri Lanka: Geologica Ultraiectina (University of Utrecht, The Netherlands), v. 114, 208 p.

Kröner, A., 1991, African linkage of Precambrian Sri Lanka: Geologische Rundschau, v. 80, p. 429-440.
Kröner, A., Braun, I., and Jaeckel, P., 1996, Zircon geochronology of anatectic melts and residues from a high-grade pelitic assemblage at Ihosy, southern Madagascar: evidence for Pan-African granulite metamorphism: Geological Magazine, v. 133, p. 311-323.
Kröner, A., Cooray, P.G., and Vitanage, P.W., 1991, Lithotectonic subdivision of the Precambrian basement of Sri Lanka, *in* Kröner, A., editor, The crystalline crust of Sri Lanka, Part I, Summary of Research of the German-Sri Lankan Consortium: Geological Survey Department of Sri Lanka Professional Paper, v. 5, p. 5-21.
Kröner, A., and Hegner, E., 1998, Geochemistry, single zircon ages and Sm-Nd systematics of granitoid rocks from the Góry Sowie (Owl) Mts., Polish West Sudetes: evidence for early Palaeozoic arc-related plutonism: Journal of the Geological Society of London, v. 155, p. 711-724.
Kröner, A., and Jaeckel, P., 1994. Zircon ages from rocks of the Wanni Complex, Sri Lanka: Journal of the Geological Society of Sri Lanka, 5, 41-57.
Kröner, A., Jaeckel, P., Reischmann, T., and Kroner, U., 1998, Further evidence for an early Carboniferous (~340 Ma) age of high-grade metamorphism in the Saxonian Granulite Complex: Geologische Rundschau, v. 86, p. 751-766.
Kröner, A., Jaeckel, P., and Williams, I.S., 1994, Pb-loss patterns in zircons from a high-grade metamorphic terrain as revealed by different dating methods: U-Pb and Pb-Pb ages for igneous and metamorphic zircons from northern Sri Lanka: Precambrian Research, v. 66, p. 151-181.
Kröner, A., Jaeckel, P., Windley, B.F., Brewer, T., and Razakamanana, T., 1999, New zircon ages and regional significance for the evolution of the Pan-African orogen in Madagascar: Journal of the Geological Society of London, v. 156, 1125-1135.
Kröner, A., Sacchi, R., Jaeckel, P., and Costa, M., 1997, Kibaran magmatism and Pan-African granulite metamorphism in northern Mozambique: Single zircon ages and regional implications: Journal of African Earth Sciences, v. 25, p. 467-484.
Kröner, A., and Sassi, F.P., 1996, Evolution of the northern Somali basement: new constraints from zircon ages: Journal of African Earth Sciences, v. 22, p. 1-15.
Kröner, A., and Todt, 1988, Single zircon dating constraining the maximum age of the Barberton greenstone belt, Southern Africa: Journal of Geophysical Research, v. 93, p. 15,329-15,337.
Kröner, A., and Williams, I.S., 1993, Age of metamorphism in the high-grade rocks of Sri Lanka: Journal of Geology, v. 101, p. 513-521.
Kröner, A., Willner, A., Hegner, E., and Nemchin, A.A., in press, Single zircon ages and Nd isotopic systematics of granulites in southern Malawi and their bearing on the extent of the Mozambique belt into southern Africa: Precambrian Research,
Lawver, L.A., Gahagan, L.M., Coffin, M.F., 1992, The development of palaeoseaways around Antarctica. The Antarctic Palaeoenvironment: A perspective on global change: Antarctic Research Series, v. 56, p. 7-30.
Lenoir, J.-L., Küster, D., Liégeois, J.P., Utke, A., Haider, A., and Matheis, G., 1994, Origin and regional significance of late Precambrian and early Palaeozoic granitoids in the Pan-African belt of Somalia: Geologische Rundschau, v. 83, p. 624-641.
Liew, T.C. and Hofmann, A.W., 1988, Precambrian crustal components, plutonic associations, plate environment of the Hercynian Fold Belt of Central Europe: Indications from a Nd and Sr isotopic study: Contributions to Mineralogy and Petrology, v. 98, p. 129-138.
Ludwig, K.R., 1994. ISOPLOT, a plotting and regression program for radiogenic-isotope data, version 2.75: United States Geological Survey, Open-File Report 91-445, 45 p.
Meert, J. G., and Van der Voo, R., 1997, The assembly of Gondwana 800-550 Ma: Journal of Geodynamics v. 23, p. 223-235.
Milisenda, C.C., Pohl, J.R., and Hofmann, A.W., 1991, Charnockite formation at Kurunegala, Sri Lanka, *in* Kröner, A., editor, The crystalline crust of Sri Lanka, Part I, Summary of research of the German-Sri Lankan Consortium: Sri Lanka Geological Survey Professional Paper, v. 5, p. 141-149.
Moine, B., 1968, Carte du Massif Schisto-Quartzo-Dolomitique. 1\200000: Antananarivo, Service Géologique de Madagasikara.
Moorbath, S., Whitehouse, M.J., and Kamber, B.S., 1997, Extreme Nd-isotope heterogeneity in the early Archean–fact or fiction? Case histories from northern Canada and West Greenland: Chemical Geology, v. 135, p. 213-231.
Mosley, P.N., 1993, Geological evolution of the late Proterozoic "Mozambique Belt" of Kenya: Tectonophysics, v. 221, p. 223-250.
Muhongo, S., Kröner, A., and Nemchin, A.A., in press, Zircon ages from granulite facies rocks in the Mozambique belt of Tanzania and implications for Gondwana assembly: Journal of Geology,
Nédélec, A., and Paquette, J.L., 1997, Age, structural setting, geochemistry and sources of late Pan-African post-collisional granitic plutonism in Madagascar: Terra Nova, v. 9, Abstract Supplement 1, p. 500.
Nédélec, A., Paquette, J.L., Bouchez, J.L., Olivier, P., and Ralison, B., 1994, Stratoid granites of Madagascar: structure and position in the Panafrican orogeny: Geodinamica Acta, v. 7, p. 48-56.
Nédélec, A., Stephens, W. A., and Fallick, A. E., 1995, The Panafrican stratoid granites of Madagascar: alkaline magmatism in a post-collisional setting: Journal of Petrology, v. 36, p. 1367-1391.
Nelson, D. R., 1997, Compilation of SHRIMP U-Pb zircon geochronology data, 1996: Geological Survey of Western Australia, Record 1997/2, 189 p.
Nemchin, A.A., Pidgeon, R.T., and Wilde, S.A., 1994, Timing of late Archean granulite facies metamorphism in the southwestern Yilgarn Craton of Western Australia: evidence from U-Pb ages of zircons from mafic granulites: Precambrian Research, v. 68, p. 307-321.
Newton, R.C., 1992, Charnockitic alteration: evidence for CO_2 infiltration in granulite facies metamorphism: Journal of Metamorphic Geology, v. 10, p. 383-400.

Newton, R.C., Smith, J.V., and Windley, B.F., 1980, Carbonic metamorphism, granulites and crustal growth: Nature, v. 288, p. 45-50.
Oliver, G.J.H., Johnson, S.P., Williams, I.S., and Herd, D.A., 1998, Relict 1.4 Ga oceanic crust in the Zambezi Valley, northern Zimbabwe; evidence for Mesoproterozoic supercontinental fragmentation: Geology, v. 26, p. 571-573.
Paquette, J.-L., and Nédélec, A., 1998. A new insight into Pan-African tectonics in the East-West Gondwana collision zone by U-Pb zircon dating of granites from central Madagascar: Earth and Planetary Science Letters, v. 155, p. 45-56.
Paquette, J.-L., Nédélec, A., Moine, B. and Rakotondrazafy, 1994: U-Pb, single zircon Pb-evaporation, and Sm-Nd isotopic study of a granulite domain in SE Madagascar. Journal of Geology, v. 102, p. 523-538.
Pidgeon, R.T., Furfaro, D., Kennedy, A., Van Bronswjk, W., and Todt, W., 1994, Calibration of the CZ3 zircon standard for the Curtin SHRIMP II: United States Geological Survey Circular 1107, p. 251.
Pinna, P., Jourde, G., Calvez, J.Y., Mroz, J.P., and Marques, J.M., 1993, The Mozambique belt in northern Mozambique: Neoproterozoic (1100-850 Ma) crustal growth and tectogenesis, and superimposed Pan-African (800-550 Ma) tectonism: Precambrian Research, v. 62, p. 1-59.
Raith, M.M., Srikantappa, C., Buhl, D., and Köhler, H., 1999, The Nilgiri enderbites, South India: nature and age constraints on protolith formation, high-grade metamorphism and cooling history: Precambrian Research, v. 98, p. 129-150.
Raymo, M.E., Ruddiman, W.F., and Froelich P.N., 1988, Influence of late Cenozoic mountain building on geochemical cycles: Geology, v. 16, p. 649-653.
Richter, F.M., Rowley, D.B., and DePaolo, D.J., 1992, Sr isotope evolution of seawater: the role of tectonics: Earth and Planetary Science Letters, v. 109, p. 11-23.
Santosh, M., Kagami, H., Yoshida, M., and Nanda-Kumar, V., 1992, Pan-African charnockite formation in East Gondwana: geochronologic (Sm-Nd and Rb-Sr) and petrologic constraints: Bulletin of the Indian Geological Association, v. 25, p. 1-10.
Shackleton, R. M., 1996, The final collision zone between East and West Gondwana; where is it? Journal of African Earth Sciences, v. 23, p. 271-287.
Shiraishi, K., Ellis, D.J., Hiroi, Y., Fanning, C.M., Motoyashi, Y., and Nakai, Y., 1994, Cambrian orogenic belt in East Antarctica and Sri Lanka: Implications for Gondwana assembly: Journal of Geology, v. 102, p. 47-65.
Silver, L.T., 1969, A geochronological investigation of the anorthosite complex, Adirondack Mountains, New York, *in* Isachsen, Y.W., editor, Origin of anorthosite and related rocks: New York Museum and Science Service Memoir, v. 18, p. 57-82.
Stern, R. J., 1994, Neoproterozoic (900-550 Ma) arc assembly and continental collision in the East African orogen: implications for the consolidation of Gondwanaland: Annual Reviews in Earth and Planetary Sciences, v. 22, p. 319-351.
Torsvik, T.H., Smeturst, M.A., Meert, J.G., Van der Voo, R., McKerrow, W.S., Brasier, M.D., Sturt, B.A., and Walderhaug, H.J., 1996. Continental break-up and collision in the Neoproterozoic and Palaeozoic–A tale of Baltica and Laurentia: Earth Science Reviews, v. 40, p. 229-258.
Tucker, R.D., Ashwal, L.D., Handke, M.J., and Hamilton, M.A., 1997, A geochronologic overview of the Precambrian rocks of Madagascar: a record from the middle Archean to the late Neoproterozoic, *in* UNESCO-IUGS-IGCP-348/368 International Field Workshop on Proterozoic geology of Madagascar: Johannesburg, South Africa, Gondwana Research Group, Proceedings, Miscellaneous Publication 5, p. 99.
Tucker, R.D., Ashwal, L.D., Handke, M.J., Hamilton, M.A., LeGrange, M., and Rambeloson, R.A., 1999, U-Pb geochronology and isotope geochemistry of the Archean granite-greenstone belts of Madagascar: Journal of Geology, v. 107, p. 135-153.
Tucker, R.D., Handke, M.J., and Ashwal, L.D., 1996, New isotopic ages and geological perspectives of the Precambrian rocks of north and north-central Madagascar: Geological Society of America, Abstracts with Programs, v. 28, p. 230.
Unrug, R., 1996, The assembly of Gondwanaland: Episodes, v. 19, p. 11-20.
Vachette, M., 1979, Radiochronologie du Précambrien de Madagascar: Colloque de Géologie Africaine, Résumés, v. 10, p. 25-27.
Vachette, M., and Hottin, A.M., 1974, Ages de 682 et de 527 Ma dans le massif granulitique de Carion (Centre de Madagascar): Comptes Rendus Académie des Sciences, Paris, v. 278, p. 1669-1671.
Whitehouse, M.J., 1989, Sm-Nd evidence for diachronous crustal accretion in the Lewisian complex of northwest Scotland: Tectonophysics, v. 161, p. 245-256.
Williams, I.S., and Claesson, S., 1987, Isotopic evidence for the Precambrian provenance and Caledonian metamorphism of high-grade paragneisses from the Seve Nappes, Scandinavian Caledonides: Contributions to Mineralogy and Petrology, v. 97, p. 205-217.
Wilson, M., 1989, Igneous petrogenesis: A global tectonic approach: London, Harper Collins Academic, 466 p.
Windley, B.F., Razafiniparani, A., Razakamanana, T., and Ackermand, D., 1994, The tectonic framework of the Precambrian of Madagascar and its Gondwana connections: a review and reappraisal: Geologische Rundschau, v, 83, p. 642-659.
Windley, B.F., and Razakamanana, T., 1996, The Madagascar-India connection in a Gondwana framework, *in* Santosh, M. and Yoshida, M., editors, The Archean and Proterozoic terranes in southern India within East Gondwana: Osaka University, Japan, Gondwana Research Group, Memoir 3, p. 25-37.